

# 1. INTRODUCTION AND EXPLANATORY NOTES, LEG 81, DEEP SEA DRILLING PROJECT<sup>1</sup>

D. G. Roberts, Institute of Oceanographic Sciences, Wormley  
J. Backman, University of Stockholm  
A. C. Morton, British Geological Survey, Keyworth, Leeds  
and  
J. B. Keene, University of Sydney<sup>2</sup>

## BACKGROUND AND PLANNING OF LEG 81

During the first International Phase of Ocean Drilling (IPOD) of the Deep Sea Drilling Project (DSDP), several passive margins were drilled in the Atlantic Ocean and the Gulf of California by means of a series of transects designed to address the evolution of passive margins in part as a function of relative age. Sites previously drilled in the northeast Atlantic during Legs 47B, 48, and 80 took advantage of reduced Tertiary progradation to facilitate safe penetration of syn- and pre-rift sediments at shallow depths. Subsequent deep seismic surveys of many margins demonstrated the importance of the northeast Atlantic as a natural laboratory for testing the problems posed by radical differences in the structural style of the various passive margins. In this area, the Bay of Biscay and Goban Spur margins are structured into a series of tilted blocks and half grabens overlain by a thin Cretaceous and Tertiary cover. In marked contrast, the southwest Rockall Plateau consists of a thick sequence of oceanward dipping reflectors; the prominent horst and graben structure of the Bay of Biscay is notably absent. Seismic surveys in other parts of the world have demonstrated the widespread occurrence of this type of margin (Hinz, 1981). The margin is closely similar to that observed beneath the outer Vøring Plateau and beneath the conjugate margin of East Greenland. During Leg 48, a first attempt was made to penetrate the dipping reflector sequence off southwest Rockall but failed because of technical difficulties (Montadert, Roberts, et al., 1979).

During Leg 81, a systematic transect of five holes across the entire west margin of Rockall Plateau was designed by the Passive Margin Panel with the specific objectives of documenting the nature of the dipping reflectors and the evolution of the margin in time and space (Fig. 1). In order to ensure maximum flexibility in the drilling program, alternate sites were proposed and accepted by the JOIDES Safety Panel to allow modification of the drilling program according to the drilling results. This was particularly useful in selecting the planned

re-entry site. The detailed objectives of Leg 81 are discussed in the site chapter for Sites 552 and 553 and individual objectives of sites in each site chapter.

## LEG 81 OPERATIONAL SUMMARY

Leg 81 of the IPOD Phase II of the Deep Sea Drilling Project began in Southampton on 27 July 1981 and ended 56 days later in Ponta Delgada, San Miguel, Azores. During the leg, *Glomar Challenger* traveled 3368.4 n. mi. and drilled eight holes at four sites. Water depths at sites ranged from 1669 to 2584 m. Hole depths ranged from 209 to 965 m. A total of 2111.5 m was cored and 1181.2 m of core recovered, representing some 55.9% (Table 1).

Time distribution for the leg was 5.10 days in port, 16.95 days cruising, and 33.83 days on site. The on-site time consisted of 6.16 days tripping, 0.67 days drilling, 16.85 days coring, 3.15 days positioning the ship, 0.02 days for mechanical downtime, 0.83 days in re-entry operations, 3.26 days waiting on weather, and 2.69 days running the down-hole logs; miscellaneous activities such as breakdowns and return to port occupied a further 3.27 days.

Leg 81 suffered a large number of weather and operational problems. The weather throughout the leg was bad. Virtually 90% of the fronts crossing the Atlantic moved through the area of operations, resulting in wind, fog, and/or rain interspersed with frontal storms at 48 hr. intervals. Although, somewhat surprisingly, only 78.2 hrs. of drilling downtime resulting from weather was logged, the weather did delay transits to and from Ireland and to the Azores, force premature abandonment of Site 554, and almost cause loss of the logging program at Site 555.

A variety of operational problems plagued the leg. At Hole 552A, VLHPC BHA was incorrectly made up with a collet head sub instead of the HPC seal sub. This necessitated a round trip and replacement of the 9.5 m barrel by the 5 m, causing delay. At Site 553, the cross bar holding the hang-off cables broke while keelhauling the re-entry cone. By miraculous efforts, the cone was hauled back on board in a 4 hr. operation. After completing the first re-entry, the vessel was notified of a medical emergency and returned to Limerick to transfer the Cruise Operations Manager and GMI Third Mate and to pick up a replacement Operations Manager. The return to Site 553 was delayed by strong headwinds and heavy seas. After re-entering Hole 553A, with

<sup>1</sup> Roberts, D. G., Schnitzer, D., et al., *Init. Repts. DSDP, 81*: Washington (U.S. Govt. Printing Office).

<sup>2</sup> Addresses: (Roberts, present address) British Petroleum Ltd., Moor Lane, London, EC2Y 9BU, United Kingdom; (Backman) Department of Geology, University of Stockholm, Stockholm, S-106 91, Sweden; (Morton) British Geological Survey, Keyworth, NG12 5GG, United Kingdom; (Keene) Dept. of Geology, University of Sydney, NSW, Australia.

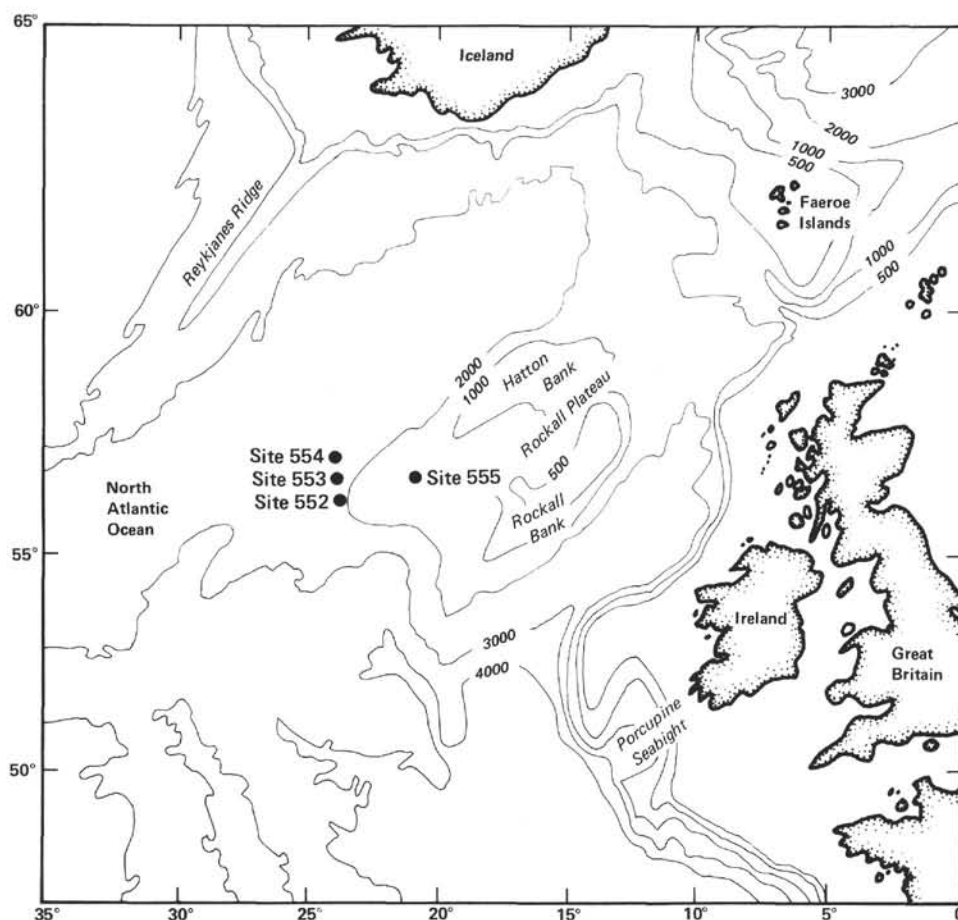


Figure 1. Map showing locations of Leg 81 drilling sites.

Table 1. Site summaries, Leg 81.

Hole	Latitude	Longitude	Water depth (m)	Number of cores	Cores with recovery	Percent of cores with recovery	Meters cored	Meters recovered	Percent recovered	Drilled	Meters	Penet.	Hole	Site
552	56°02.56'N	23°13.39'W	2315	25	21	84.0	219.0	79.19	36.2	95.0	314.0	22.0	69.2	
552A	56°02.56'N	23°13.39'W	2311	38	38	100.0	183.5	182.97	99.7	—	183.5	HPC	89.7	158.9
553	56°05.32'N	23°20.61'W	2339	1	1	100.0	9.0	8.33	92.6	50.5	59.5	300.0	22.0	
553A	56°05.32'N	23°20.61'W	2339	59	59	100.0	531.5	288.97	54.4	151.0	682.5	27.0	290.4	
553B	56°05.32'N	23°20.61'W	2338	4	4	100.0	33.5	33.23	99.2	—	28.5	HPC	25.1	337.5
554	56°17.41'N	23°31.69'W	2584	8	7	87.5	76.0	53.76	70.7	—	76.0	81.4	26.5	
554A	56°17.41'N	23°31.69'W	2584	14	14	100.0	133.0	29.52	22.2	76.0	209.0	28.1	41.7	68.2
555	56°33.70'N	20°46.93'W	1669	98	97	99.0	926.0	505.25	54.6	38.0	964.0	16.4	245.9	245.9
Leg totals				247	241	97.6	2111.5	1181.22	55.9	410.0	2517.0	18.4	810.5	810.5

difficulty as a result of damage to the reflectors on the cone, drilling went ahead without difficulty until Core 59 when the HBR prematurely released in the hole. Since there was no way of fishing the lost bit, the logging program was initiated and successfully completed. A further attempt was made to VLHPC Hole 553A, but the device jammed and the hole had to be abandoned. At Hole 553B, a further attempt was made to VLHPC but again failed when the barrel stuck and could not be dislodged. Site 554 was interrupted by a period of bad weather and was drilled as two holes. Hole 554A was abandoned finally because of difficult drilling condi-

tions. Site 555 was drilled under continually deteriorating weather conditions and also encountered several technical problems. The first attempt to spud the hole failed when the HBR shifted, releasing the bit in midwater. After reaching basement at 965 m, the weather deteriorated markedly so the logging program was delayed pending an improvement. During the weather delay, the hole had bridged at several points, and it was only with great difficulty and endeavor that the hole was cleaned to allow a successful logging program just prior to a complete deterioration in the weather. Poor weather conditions persisted nearly all the way to the Azores.

The performance of the dynamic positioning system was excellent and was severely tested under the adverse weather conditions. One beacon failure occurred. Radio communications were poor throughout the leg.

### SUMMARY OF SCIENTIFIC RESULTS

Detailed scientific results at each site are reported in the site chapters, this volume. A brief general synopsis has been previously published (Scientific Staff, 1982). At the end of this volume, a series of chapters synthesize the results of the cruise in terms of the major problems of the dipping-reflector type of margin and regional aspects of North Atlantic stratigraphy and paleoceanography.

The following section offers a brief synopsis of the major scientific results at each site.

### PRINCIPAL RESULTS

#### Sites 552 and 553

Sites 552 and 553 were the midpoint of the drilling transect and were drilled to penetrate the dipping reflectors so as to establish their age and origin as well as the subsidence history of the margin. Hole 552 was drilled to total depth in basalt of 282.7 m when bad weather caused abandonment; three heat-flow measurements were made. Hole 552A was hydraulically piston cored to 183.5 m, yielding almost 100% recovery. Hole 553 was drilled as a pilot hole for re-entry Hole 553A. Three heat-flow measurements and two successful re-entries were made at Hole 553A before the bit fell off, aborting the hole at 682.5 m; the hole was logged with all tools. Hole 553B was an abortive attempt to repeat the successful HPC at Hole 552A. Sites 552 and 553 are complementary, and the principal results are here summarized together.

A complete Pliocene–Pleistocene section (44 m) was cored at Hole 552A. Deposition took place in water depths comparable to those at present at an average rate of 1.4 cm/1000 yr. Above 44 m, a strong cyclical variation in lithology is present and represents glacial–interglacial cycles; a complete Pliocene–Pleistocene record was recovered at the site. Sedimentation was continuous between the Miocene and Oligocene only at Hole 553A where a thin (4 m) nannofossil chalk represents the early Miocene. A hiatus encompassing NN2–NN4 separates the early Miocene (NN1) from the overlying early Miocene (NN5) glauconitic foraminiferal chalk. At Hole 552A, the early Miocene is absent and the Oligocene is succeeded by middle Miocene (NN7) glauconitic foraminifer chalk. A middle Miocene hiatus is present at both sites. Water depths of deposition of greater than 2000 m are comparable to those at present.

The late(?) Eocene–Oligocene interval at both sites comprises a condensed sequence (maximum 1.75 m) containing several hiatuses that bridge the 30 m.y. of geological time between the middle Eocene and the early Miocene. At Hole 553A, 0.75 m of late Oligocene chalk with palagonitized ash rests on the middle Eocene. Manganese nodules and fish remains at the base suggest a period of prolonged nondeposition and/or erosion. At

Hole 552A, a more complete section was cored using the HPC. At this site, the Oligocene section (1 m) contains Zones NP21–24 compared to NP25 at Site 553. Depths of deposition in Oligocene time increased from about 700 m to in excess of 1400 m in late Oligocene time. A large part of the middle Eocene is missing at both Site 552 and Hole 553A. The section at both sites consists of pale brown biosiliceous nannofossil–foraminifer chalk deposited in water depths exceeding 700 m.

Sediments of early Eocene age were found overlying the basalt at Sites 553 and 552. At Site 552, only 108.5 m of early and middle Eocene (Zones NP11–16) was present in comparison to 264.52 m of early and middle Eocene sediments (NP10–16) at Site 553. Biostratigraphic and heavy mineral correlation shows that the whole of Unit IV at Site 552 is equivalent to Unit IVb of Site 553. In contrast, the underlying 227.85 m of section at Site 553 is absent at Site 552 but possibly underlies the basalt cored at total depth. For convenient review, the lowermost subunits (IVc to IVf) of Hole 553A are described first.

At Hole 553A, Subunit IVf sediments overlying the basalt are of NP10 age and reversely magnetized, indicating deposition during the reversed polarity interval between Anomalies 24 and 25. Those sediments consist of sandy tuffaceous mudstones succeeded by tuffaceous mudstones deposited in depths that shoaled from inner shelf to brackish marsh. The succeeding Subunit IVc was deposited in inner shelf depths and consists of volcanic lapilli, altered glass, and zeolites. The few fragments recovered of Subunit IVd consist of arkosic sandstones deposited in inner to mid-shelf water depths. Subunit IVc is marked by a sharp increase in the abundance of tuffs that are more silicic than Subunits IVe and IVb. The first appearance of an early Eocene nannoflora (NN10/11 boundary) occurs near the base of the unit and lies within a normal polarity interval. A heavy mineral assemblage characterized by metamorphic hornblende and epidote is present throughout. Depths of deposition ranged from lagoonal or estuarine to inner shelf. The top of the unit is placed beneath a highly glauconitic unit marking a major marine transgression. The succeeding Subunit IVb is marked by the appearance of nannofossil chalk, interbedded with and containing reworked vitric tuffs. Benthic foraminifers indicate a depth change from 100 to 180 m to greater than 700 m by NP14 time. At Site 552, the thicker IVb equivalent has an age range of NP11 at the base to NP14 at the top. The basal section (Subunit IVa) of terrigenous diatomaceous claystone is succeeded by glauconitic sediments (Subunit IVc) deposited in depths of 75–100 m. The overlying subunit (IVb) consists of volcanic ash and tuffaceous chalk deposited in mid-outer shelf depths.

Basaltic lava flows were recovered at Holes 552 and 553A. At Site 552, only 7.95 m of deeply altered, reversely magnetized basalt was cored. The basalt is believed to be submarine and younger (late NP10/early NP11) than the basalts cored at Hole 553A.

At Hole 553A, 181.5 m of basalt were drilled and cored to total depth at 682.5 m. Thirty-four lava flows were identified from the logs and 27 were recognized in

the cores. Typical flow units consist of a weathered scoriaceous agglomeratic top passing gradationally downward into vesicular basalt, massive basalt, and into the highly vesiculated base of the flow. Petrographic and geochemical studies show the basalts to be essentially uniform in composition, tholeiitic and of MORB affinity. Three basalt subunits were identified from the physical properties data, downhole logs, and paleomagnetic measurements; zones of high gamma response, high porosity, low sonic velocity and density may indicate interbedded sediment. Paleomagnetic measurements show that all the basalts are reversely magnetized but also show distinct cyclical variations in inclination tentatively interpreted as secular variation. Age determinations on the basalt of  $53.5 \pm 1.9$  m.y. indicate eruption in the Anomaly 24–25 reversed polarity interval.

#### Holes 554/554A

Site 554 was drilled to examine the nature and origin of the outer high forming the western boundary of the suite of oceanward dipping reflectors at the base of Rockall Plateau. The high is located in the region of the possible continent/ocean boundary shown by the partial overlap of Anomaly 24B with the high. Additional objectives included an assessment of the subsidence history of the high and its paleodepth in relation to the dipping reflector sequence to the east and the oceanic crust to the west during rifting and later drifting. The site was drilled and cored to a depth of 209 m and was abandoned at this depth because of difficult drilling conditions. Two heat-flow measurements were made. No logging could be done.

Five lithologic units were recognized: Unit I (0 to c. 28.5 m) is composed of Quaternary to late Pliocene foraminiferal–nannofossil oozes and muds deposited in present-day water depths. The base of the unit is indeterminate and lies in a zone of zero recovery. Unit II (c. 28.5 to 106.0 m) is of early Pliocene to middle Miocene age and consists of foraminiferal–nannofossil oozes which grade to chalk below 95 m. Water depths were in the range of 2200–2900 m.

Unit III consists of two subunits. Subunit IIIa (106.0 to 106.25 m) is of early Miocene age and is characterized by pale yellow to olive gray glauconitic nannofossil–foraminiferal or foraminiferal chalks. The top of the unit is marked by a hiatus below the middle Miocene; a marked hiatus is probably present at the base of the subunit. Subunit IIIb (106.25 to 118.80 m) is of Oligocene to late Eocene. It is characterized by yellow glauconitic foraminiferal chalks and marls with a downward increase in glauconite. The base of the subunit is marked by a 10 cm thick manganese layer which rests on early Eocene sediments of Unit IV. The condensed Oligocene–late Eocene sequence (12.5 m of sediment representing 15 m.y.) is remarkable in that part of all the nannofossil zones between NP25 and NP19/20 are present. Water depths were probably about 700 m. A hiatus of about 12 m.y. separating the late Eocene and early Eocene defines the base of the subunit.

Unit IV (118.80 to 126.60 m) is of early Eocene age. The top of the unit is an unconformity below the man-

ganese layer; the base is defined by the change to conglomerate. The unit consists of yellowish brown to dark brown tuffaceous marlstones and tuffs deposited in water depths of 100–150 m near the top of the unit and 75–150 m near the base.

Unit V (126.60 m to 209.0 m) is of probable early Eocene age and consists of normally magnetized volcanogenic conglomerates and sandstones interbedded with normally magnetized basaltic lava flows. The conglomerate contains rounded and angular clasts of basalt and lies in erosional contact with the underlying basalt; the conglomerate may represent a transgressive pebble beach. At least six basalt flows are present; their characteristics are compatible with eruption in a shallow submarine environment followed by low temperature alteration.

#### Site 555

Site 555 was located on the flank of the shallow Hatton and Edoras banks which together make up the western culmination of the Rockall Plateau and the most “landward” part of the dipping reflector sequence. In the vicinity of the site, subhorizontal basement reflectors are present. Our objective at the site was to penetrate the subbasement reflectors and, by comparison of the subsidence history of the site with that obtained at the sites in the dipping reflector sequence and on the outer high, to assess the relative roles of rift and postrift subsidence in fashioning the observed structural relief. Five heat-flow measurements were made at the site, and the larger part of the hole was logged despite considerable difficulty.

Four lithologic units were distinguished: Unit I (0–22.3 m) of Quaternary age is characterized by alternating horizons of ooze, marls, and calcareous muds. The base of the unit is marked by a hiatus between Pleistocene sediments and earliest Pliocene sediments. Unit II (22.3 to 281.0 m) consists of pelagic sediments of early Pliocene to early Miocene age and two subunits are distinguished: a small hiatus between the early and middle Miocene is present in Core 24. Water depths of deposition were about 1500 m. The base of the unit is defined by a major Miocene–Eocene unconformity separating the pelagic chalks from the volcanogenic Eocene sequence below.

Unit III (281.0 to 672.3 m) is of early Eocene age and consists of a wide variety of lithologies transitional between Unit II and the interbedded lavas and volcanogenic sediments of Unit IV (672.3 to 964.0 m) of late Paleocene age. Units III and IV mark the waning of volcanism and onset of subsidence associated with the transition from rifting to spreading and are here summarized together. The basalts drilled from 927.0 to 964.0 m total depth make up a single massive flow unit. Eleven flow units identified in the overlying basalts consist of single and composite tholeiitic pillow lava units. Interbedded with the basalts are 47 m of autoclastic/hyaloclastite breccias with thin intercalations of sediment. These sediments show reverse polarity and are of late Paleocene (NP9) age. Typical lithologies are tuffs and lapilli tuffs interbedded with poorly sorted micaceous and feldspathic sandstones. The overlying sediments of Unit

IIIe are of reverse polarity and NP10 age (632.5 to 672.3 m); they rest with sharp contact on the basalt and consist of vitric tuffs, lapilli tuffs with minor interbeds of sandstones and mudstones; benthic foraminifers indicate inner shelf depths. These primarily volcanogenic sediments pass upward into Subunit IIId (482.5 to 632.5 m) of late Paleocene age. The predominant facies is a brownish black mudstone; benthic foraminifers show an upward decrease in depth of deposition from inner shelf (Core 61) to brackish intertidal marsh by Core 52. Subunit IIId is considered equivalent to lithologic Unit IVa from Site 553. Subunit IIIC (352.2 to 482.5 m) comprises a series of volcanic tuffs and lapilli tuffs interbedded with carbonaceous mudstones and highly feldspathic sandstones of NP10 age. Intermediate to acidic tuffs indicate a comparison with Subunit IVc of Site 553. The transition from Subunit IIIC to IIIB (320.0 to 352.2 m) is marked by the appearance of abundant glauconite. Subunit IIIB is of reverse polarity and NP10 age in its lower part but of normal polarity and NP11 age at the top. Tuffaceous glauconitic sandstones characterize the unit and may represent the same major transgressive unit observed at the base of Subunit IVb of Site 553. The base of the unit is marked by the upward disappearance of the Greenland epidote-amphibole heavy mineral assemblage, but heavy minerals derived from the metamorphic basement of Rockall occur throughout. Benthic foraminifers show an increase in water depth of deposition from 25–100 m to 100–200 m. The increase in water depths coincident with the occurrence of Anomaly 24B in the upper part of the unit suggests that the major transgression is coincident with the rift/drift transition at about Anomaly 24B time. The overlying Subunit IIIa (281.0 to 320.0 m) is characterized by lithologies such as spiculite, zeolitic chalk, vitric tuff, and bioclastic limestone transitional to those of overlying Unit II. The sediments are of NP11 age and were deposited in increased water depths of 150–200 m.

## EXPLANATORY NOTES

### Responsibility for Authorship

The shipboard party collectively authored the site chapters; ultimate responsibility lies with D. G. Roberts who rewrote much of these chapters and J. Backman who rewrote and coordinated the biostratigraphic sections. Chapters 2 through 4 present data and discussions on the holes drilled. However, presentation of the site chapters does not necessarily follow the format previously established in DSDP volumes. In Chapters 2 through 4, Sites 552 and 553 have been grouped together. The remaining sites are discussed in individual chapters. All site chapters, however, follow the same general outline (below), with the authorship listed in parenthesis.

#### Site Data and Principal Results

#### Background and Objectives (Roberts)

#### Operations (Roberts)

#### Lithology (Keene, Morton, Desprairies, Zimmerman, Roberts)

#### Biostratigraphy (Backman, Baldauf, Murray, Westberg-Smith)

#### Biostratigraphic Summary (Backman)

#### Foraminifers (Huddleston, Murray)

#### Calcareous Nannofossils (Backman)

#### Diatoms (Baldauf)

#### Radiolarians (Westberg-Smith)

#### Palynology (taken from shoreside studies)

#### Physical Properties (R. Homrighausen)

#### Correlation of Seismic Reflectors (Roberts)

#### Sedimentation Rates (Backman)

#### Summary and Conclusions (Roberts, Backman)

Severe time restrictions were placed on the preparation of these site chapters. Ordinarily, extensive use would have been made of studies made post-cruise by shipboard and shoreside scientists to ensure that the site chapters were fully complete, accurate, and consistent. However, in preparing the site chapters only very preliminary results were available, and we therefore regret any unintentional inconsistencies that may have arisen. The site chapters should therefore be read in conjunction with the fuller reports found later in the volume. Contributions made by individual shoreside workers to sections of the site chapter are fully acknowledged.

Chapters in the volume are grouped under paleontology, sedimentology, organic geochemistry, and into a series of synthesis chapters designed to provide an overview of the dipping reflector problem and North Atlantic paleoceanography. Shipboard organic geochemical and inorganic geochemical data are discussed in the site chapters as well as in individual chapters by Kaltenback and Gieskes.

We regret that several chapters originally scheduled for the volume could not be included because of time restrictions. Some of these results have been included in the synthesis chapters, and it is hoped that they will be subsequently published in the open literature.

### Survey and Drilling Data

The survey data used for specific site selections are given in each site chapter. On passage between sites, continuous observations were made of depth, magnetic field, and sub-bottom structure. Short surveys were made on *Glomar Challenger* before dropping the beacon, using a precision echo-sounder, seismic profiles, and magnetometer.

Underway depths were continuously recorded on a Giffit precision graphic recorder (PGR). The depths were read on the basis of an assumed 800 fathoms/s sounding velocity. The sea depth (in m) at each site was corrected (1) according to the tables of Matthews (1939) and (2) for the depth of the hull transducer (6 m) below sea level. In addition, any depths referred to the drilling platform have been calculated under the assumption that this level is 10 m above the water line.

The seismic profiling Teledyne system consisted of two Bolt air guns, a hydrophone array, Bolt amplifiers and filters, and two EDO recorders which had the same filter settings.

### Drilling Characteristics

Since the water circulation down the hole is an open one, cuttings are lost onto the sea bed and cannot be examined. The only information available about sedimentary stratification between cores, other than from seismic data, is from an examination of the behavior of the

drill string as observed on the drill platform. The harder the layer being drilled, the slower and more difficult it is to penetrate. However, there are a number of other variable factors which determine the rate of penetration, so it is not possible to relate this directly with the hardness of the layers. The parameters of bit weight and rpms are recorded on the drilling recorder and influence the rate of penetration which is recorded on the superlogs.

### Drilling Disturbances

When the cores were split, many showed signs that the sediment had been disturbed since its deposition. Such signs were the concave downward appearance of originally plane bands, the haphazard mixing of lumps of different lithologies, and the near fluid state of some sediments recovered from tens or hundreds of meters below the sea bed. It seems reasonable to suppose that these disturbances came about during or after the cutting of the core. Three different stages during which the core may suffer stresses sufficient to alter its physical characteristics from those of the *in situ* state are: cutting, retrieval (with accompanying changes in pressure and temperature), and core handling.

### Shipboard Scientific Procedures

#### Numbering of Sites, Holes, Cores, Samples

Drill site numbers run consecutively from the first site drilled by *Glomar Challenger* in 1968; the site number is thus unique. A site refers to the hole or holes drilled from one acoustic positioning beacon. Several holes may be drilled at a single locality by pulling the drill string above the seafloor ("mud line") and offsetting the ship some distance (usually 100 m or more) from the previous hole.

The first (or only) hole drilled at a site takes the site number. Additional holes at the same site are further distinguished by a letter suffix. The first hole has only the site number; the second has the site number with suffix A; the third has the site number with suffix B; and so forth. For example, if Site 553 had three holes drilled, they should be referenced as Site 553 (first hole), Hole 553A (second hole), and Hole 553B (third hole). It is important, for sampling purposes, to distinguish the holes drilled at a site, since recovered sediments or rocks usually do not come from equivalent positions in the stratigraphic column at different holes.

The cored interval is the interval in meters below the seafloor measured from the point at which coring for a particular core was started to the point at which it was terminated. This interval is generally 9.5 m (nominal length of a core barrel) but may be shorter if conditions dictate. Cores and cored intervals need not be contiguous. In soft sediment, the drill string can be "washed ahead" without recovering core by applying sufficiently high pump pressure to wash sediment out of the way of the bit. In a similar manner, a center bit, which fills the opening in the bit face, can replace the core barrel if drilling ahead in hard sediments without coring is necessary.

The maximum (full) core recovery in a single coring attempt is 9.5 m of sediment or rock (Fig. 2). This consists of 9.3 m in a plastic liner that is held within the core barrel, and 0.2 m in the core catcher which is screwed onto the lower end of the barrel. When a core is brought on board, the plastic liner and core are cut in 1.5 m sections starting from the top of the recovered sediment. A full 9.5 m core thus consists of six full 1.5 m sections numbered 1 to 6 from the top down, a short (0.3 m) Section 7, and the core catcher at the bottom (see discussion below concerning logging of the core catcher). In the case of partial recovery (Fig. 2), sections still are measured off and numbered from the top of the recovered sediment; however, the number of sections will correspond to the number of 1.5 m intervals necessary to accommodate the length of core recovered. This may range anywhere from 1 to 6, with the lowermost section usually containing less than 1.5 m and the core catcher.

On Leg 81, the core-catcher samples were split, then logged on the barrel sheets and stored as an additional increment (maximum 0.2 m) of sediment at the bottom of the lowermost section of each core. Despite some contrary opinions, an attempt also was made to maintain the nonconventional designation of "CC" for the catcher samples. The full designation of catcher samples from this leg thus includes the number of the lowermost section of the core within which the catcher was logged; for example, 553A (site and hole); 52 (core number); 5 (section number); CC.

The cores taken from a hole are numbered sequentially from the top down as the coring proceeds. By DSDP convention, the top of the recovered sediment (top of Section 1) is assigned the depth of the top of the cored interval and any unrecovered sediment is represented as a void at the bottom of the cored interval (Fig. 2). The core number and its associated cored interval in meters below the seafloor are unique for a hole and are entered into the DSDP computerized data base.

In the core laboratory on *Glomar Challenger*, after routine processing, the 1.5 m sections of sediment core and liner are split in half lengthwise. One half is designated the "archive" half, which is described by the shipboard geologists, and photographed; the other is the "working" half, which is sampled by the shipboard sedimentologists and paleontologists for further shipboard and shore-based analyses.

Samples taken from core sections are designated by the interval in centimeters from the top of the core section from which the sample was extracted; the sample size, in cm<sup>3</sup>, is also given. Thus, a full sample designation would consist of the following information:

Leg (optional)

Site (hole, if other than first hole)

Core number

Section number

Interval in centimeters from top of section

Hole 553A-52-3, 122-124 cm (10 cm<sup>3</sup>) designates a 10 cm<sup>3</sup> sample taken from Section 3 of Core 52 from the second hole (A) drilled at Site 553. The depth below the seafloor for this sample would be the depth to the top of

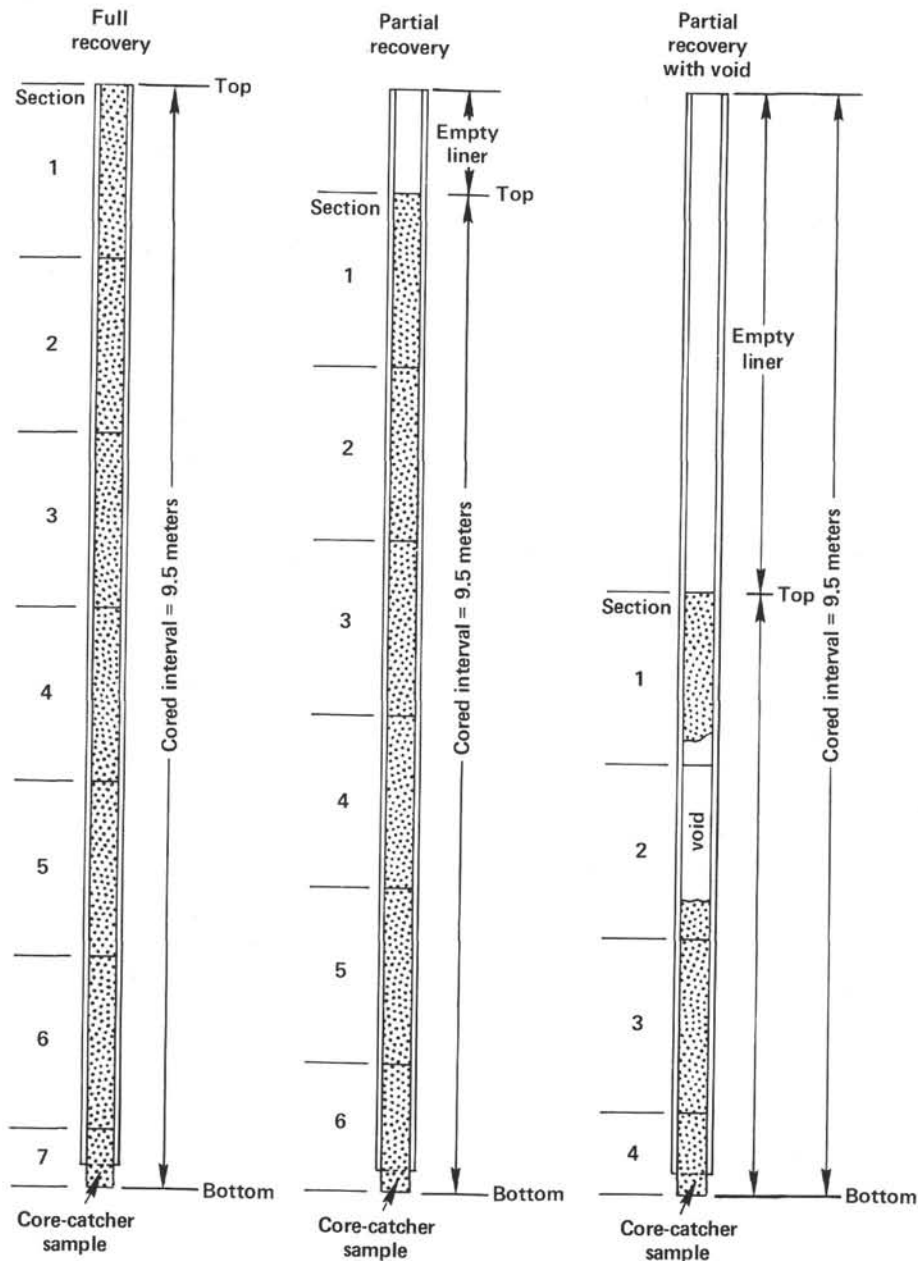


Figure 2. Diagram showing procedure in cutting and labeling of core sections.

the cored interval (in this case 559 m) plus 3 m for Sections 1 and 2, plus 122 cm (depth below top of Section 3), or 563.22 m.

### Core Handling

The first assessment of the core material was made on samples from the core catcher.

After a core section had been cut, sealed, and labeled, it was brought into the core laboratory for processing. The routine procedure listed below was usually followed.

1. Weighing of the core section for mean bulk density measurement;
2. GRAPE analysis for bulk density;

3. Sonic velocity determinations;
4. Thermal conductivity measurements.

After the physical measurements were made, the core liner was cut, and the core split into halves by a wire cutter if the sediment was a soft ooze. If compacted or partially lithified sediments were included, the core was split by a machine band saw or diamond wheel.

One of the split halves was designated a working half. Samples, including those for grain-size, X-ray mineralogy, interstitial water chemistry, and total carbon, organic carbon, and carbonate content were taken, labeled, and sealed. Larger samples were taken from suitable cores for organic geochemical analysis, usually prior to splitting the core. The working half was then sampled for shipboard and shore-based studies.

The other half of a split section was designated an archive half. The cut surface was smoothed with a spatula to emphasize the sedimentary features. The color, texture, structure, and composition of the various lithologic units within a section were described on standard visual core description sheets (one per section), and any unusual features noted. A smear slide was made, usually at 75 cm if the core was uniform. However, two or more smear slides were often made for each area of distinct lithology in the core section. The smear slides were examined under a petrographic microscope. The archive half of the core section was then photographed, both in color and in black and white. Both halves were sent to cold storage on board ship after they had been processed.

Material obtained from core catchers, and not used up in the initial examination, was retained for subsequent work in freezer boxes. Sometimes significant pebbles from the cores were extracted and stored separately in labeled containers.

All samples recovered on Leg 81 are now deposited in cold storage at the DSDP East Coast Repository at Lamont-Doherty Geological Observatory and are available to investigators.

## Procedures Used in the Measurement and Presentation of Physical Property Data

### Objectives

Physical properties data derived from cores help the shipboard selection and interpretations of sediment units and aid correlation of those units with downhole logs and with seismic reflectors, thereby providing a means of extrapolating information beyond the drill sites. With this purpose in mind the two primary objectives consisted of (1) relating physical properties of cores to lithology, with emphasis on composition and lithification (including compaction and cementation) and (2) correlating lithology to downhole logs.

### Sampling and Measurements

Physical properties determinations on cores (in addition to coring rate) include: temperature, sound speed, wet-bulk density, sound impedance, porosity, water content, and a few measurements of shear strength made with the vane-shear equipment on uncompacted sediment within the top 160 m below the ocean bottom. Brief descriptions of procedures for sampling and measurement follow. The reader may consult detailed discussions in the various shipboard manuals and the publication by Boyce (1976).

Understanding relationships among physical properties and lithologies requires close coordination between sample selection and description of lithology while in progress on board ship; selection of samples to avoid drilling disturbance and fractures; careful preparation of samples; and use of the same interval (of 5 to 10 cm), slab, or plug (minicore) for sound speed, bulk density, porosity, and water content as well as  $\text{CaCO}_3$  content. Immediate calculation of sound speed allowed recognition of changes in lithology, more critical examination

of the core, and selection of more samples for definition of key beds that might help correlation with downhole logs. Measurements of sound speed (with the Hamilton Frame) and wet-bulk density (by the two-minute GRAPE method) on two samples per section when plotted relative to depth produced logs with striking accord to the lithologic observations and the downhole logs.

Temperature measurements merely involved inserting a thermometer into the sediment of the split liner at the time of sample selection, immediately prior to measurement of sound speed.

Measurements of compressional sound speed with the Hamilton Frame ranged from an average of two per core at the beginning of the cruise (Site 552) up to ten per core at the end of the cruise (Site 555). The more frequent measurements reflected delineation of abrupt velocity changes. Techniques included measurement of uncompacted sediment in the split liners, measurement on slabs of compact sediment removed from the liners and squared with a razor or saw, and measurements on plugs (minicores) cut with the drill press.

Except in the uncompacted sediment, sound speeds were determined both parallel and perpendicular to the sediment layers.

Measurements of wet-bulk density utilized the Gamma Ray Attenuation Porosity Evaluator (GRAPE) and the weight/volume procedures in the shipboard chemistry laboratory. Before the cores were split, selected sections, which most nearly filled the plastic liners, were run through the continuous GRAPE equipment. In uncompacted sediment the two-minute GRAPE measurements utilized metal cylinders (Boyce bottles) or the split plastic liner, whereas the weight/volume determinations came from small syringe samples. In compact sediment, two-minute GRAPE measurements and weight/volume determinations both came from the same slabs or plugs utilized for the sound speed measurements.

Determinations of wet-bulk density, porosity, and water content in the shipboard chemistry laboratory averaged two per core. These determinations utilized the same samples measured with the Hamilton Frame and with the GRAPE.

### Calculation and Data Tables

Each of the site chapters that follows includes a numerical summary of physical properties determinations plotted relative to core interval and sub-bottom depth, including general lithology and  $\text{CaCO}_3$ . The data tables vary somewhat from chapter to chapter.

Determinations of sound speed anisotropy and impedance involve simple calculations. The anisotropy appears as a numerical difference between values measured parallel and perpendicular to the sediment layers, and as a percentage difference between the two. Calculations of sound impedance (sound speed  $\times$  wet-bulk density) include two forms for comparison: one using an average of densities determined by the two-minute GRAPE and the other using the weight/volume data for density. Both calculations utilize the sound speeds measured parallel to the sediment layers on the assumption that these would most nearly equal *in situ* sound speeds,

allowing for expectable decrease in sound velocity due to unloading in bringing the core to the surface. This assumption apparently was incorrect for some well-cemented rocks because the sound speeds measured perpendicular to the sediment layers with the Hamilton Frame agreed with the downhole sound speeds also measured perpendicular to the beds.

The  $\text{CaCO}_3$  percentages in the physical properties summaries were derived in the shipboard chemistry laboratory by the carbonate bomb method used on the same samples on which physical properties were derived.

### Downhole Logging

Downhole logging is perhaps best known for its use in petroleum exploration, where it is widely and successfully used in correlation and stratigraphic studies and in the evaluation of formation fluids and lithology. In deep-sea drilling, the importance of logging is both great and obvious in determining *in situ* sonic velocities to accurately correlate seismic reflectors with lithology, to compare the shipboard determination of physical properties with those measured *in situ*, and to determine lithologies in areas of poor recovery.

The principles of downhole logging and its practice on board *Glomar Challenger* are discussed here to avoid repetition in each site chapter. Interpretations of the downhole logs are given in each site chapter.

### Principles of Downhole Logging

The following tools were on board *Glomar Challenger* for Leg 81:

1. Compensated Neutron Log (CNL)—3 3/8 in. O.D.
2. Sonic (BHC)—3 3/8 in. O.D.
3. Compensated Formation Density (FDC)—3 3/8 in. O.D.
4. Gamma Ray (GR)—3 3/8 in. O.D.
5. Variable Density Log (VDL)—3 3/8 in. O.D.
6. Induction Resistivity (ISF)—3 3/8 in. O.D.
7. Temperature Log—1 11/16 in. O.D.

The brief explanation given here of the principles of operation of each tool is based on Schlumberger Log Interpretation v. I—Principles (1972).

### Compensated Neutron Log (CNL)—Porosity Log

The compensated neutron log (CNL) is used principally for the delineation of porous formations and the determination of their porosity.

A radioactive plutonium-beryllium or americium-beryllium source mounted in the sonde continuously emits neutrons. These neutrons collide with nuclei in the sediment and lose energy with each collision. The quantity of energy lost per collision is dependent on the relative mass of the nucleus with which the neutron collides. The greatest loss occurs when the neutron strikes a hydrogen nucleus. The deceleration of the neutrons is therefore dependent on the amount of hydrogen in the formation. Successive collisions decelerate within microseconds the neutrons to thermal velocities corresponding to energies of around 0.25 electron volts. The neutrons then diffuse randomly without further energy loss until captured by the nuclei of atoms such as hydrogen, sili-

con, chlorine, etc. On excitation these nuclei emit high-energy gamma rays or neutrons.

The CNL measures these neutron activities at detectors  $N_1$  and  $N_2$ , spaced at 16 and 24 in. from the source (Fig. 3). The ratio of the counting rates at these detectors is related to the quantity of hydrogen and hence to the liquid-filled pore space of the formation. The ratio is processed by a surface computer to yield a linearly scaled recording of neutron porosity index that assumes a limestone matrix.

The counting rates at the detectors fluctuate even where the porosity is constant because the collisions are random. The count rates are therefore averaged in a time-constant circuit. The appearance and statistical accuracy of the log are therefore functions of the setting of the time constant and the logging speed. A time constant of 2 s and a logging speed of 1800 ft./hr. yield good quality logs.

It should be noted that the CNL detects all of the water in the formation and not the interstitial water alone. For example, it detects water chemically bonded to shales. In such formations, the neutron porosity is greater than the effective porosity. Minor corrections to the CNL for borehole size, salinity, temperature, and pressure can be derived from nomograms.

### Sonic Log (BHC)

The sonic log is a recording, versus depth, of the time ( $\Delta t$ ) required for a compressional sound wave to traverse 1 ft. of formation. The interval transit time is the reciprocal of the velocity of the compressional sound wave and is dependent on the lithology and porosity of the formation.

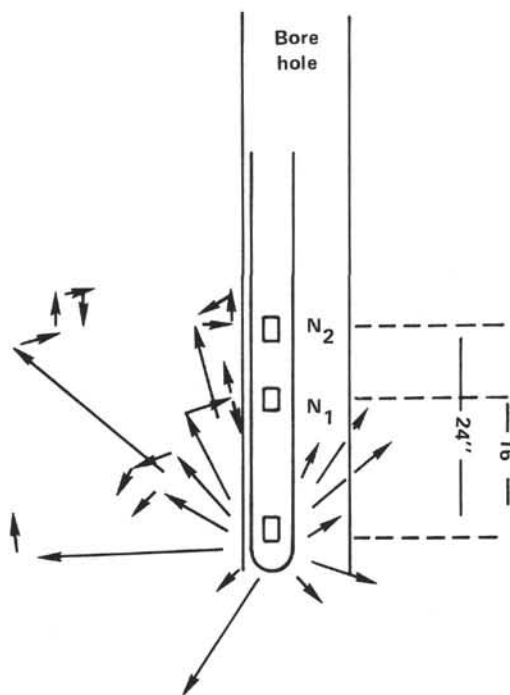


Figure 3. Schematic of the compensated neutron log used principally for delineation of porous formations.

The Borehole Compensated Log (Fig. 4) consists of two pairs of receivers with a transducer above and below. The elapsed time between transmission of a sound pulse and detection of the first arrival at the two corresponding receivers is measured continuously. As the speed of sound in the sonde and borehole fluid is less than that of the formation, the first arrival corresponds to a wavelet that has traveled through the formation.

The transducers are pulsed alternately and the  $\Delta t$  values read on the pairs of receivers. These values are automatically averaged by computer to cancel errors resulting from sonde tilt and changes in hole size. The transit time is also integrated by computer to give the total travel time to aid seismic interpretation.

Occasionally, a weak first arrival may only trigger the first receiver and the second receiver may be triggered by a later arrival in the same wave train. Spuriously large travel times thus measured in pulse cycles are shown on the sonic curve as excursions towards higher  $\Delta t$  values, known as cycle skipping. This phenomenon is likely to occur when the signal is strongly attenuated by unconsolidated or heavily fractured formations.

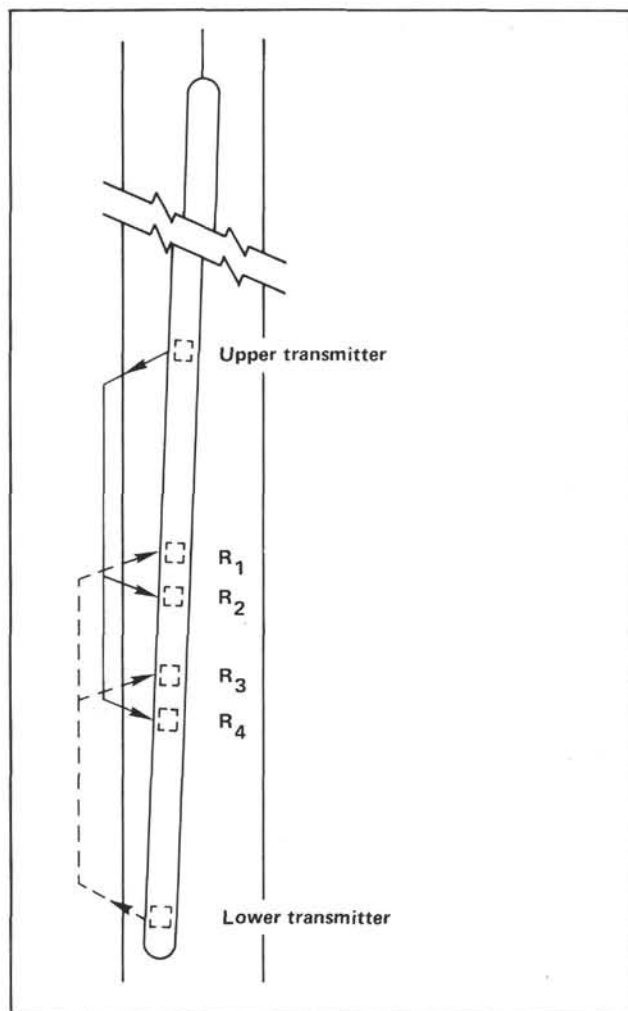


Figure 4. Schematic of BHC sonde, showing ray paths for the two transmitter-receiver sets. Averaging the two  $\Delta t$  measurements cancels errors resulting from sonde tilt and hole-size changes.

The  $\Delta t$  data are displayed in units of microseconds per foot together with the gamma and caliper logs. The integrated travel time is given by a series of pips recorded at millisecond intervals.

The transit time data can be used to evaluate porosity (Wyllie, 1956, 1958) according to the relation:

$$\frac{\Delta t_{\log} - \Delta t_{ma}}{\Delta t_f - \Delta t_{ma}}$$

where

- $\Delta t_{\log}$  = sonic log value in microseconds per ft.,
- $\Delta t_{ma}$  = transit time of the matrix material,
- $\Delta t_f$  = about 189 s/ft. (corresponding to a "fluid velocity,"  $v_f$ , of about 5300 ft./s).

### Compensated Formation Density (FDC)

The Formation Density Log provides direct measurements of density and is useful as a porosity logging tool.

The tool consists of a radioactive source which is applied to the borehole wall in a shielded sidewall skid (Fig. 5). The source emits medium-energy gamma rays which lose energy as they undergo Compton scattering by the electrons in the formation. The number of Compton scattering collisions is related directly to the number of electrons in the formation. Gamma rays reaching the detector at a fixed distance from the source are counted and give a measure of the electron density or number of electrons per cubic centimeter of the formation. Electron density is related to the true bulk density,  $\rho_b$  grains/

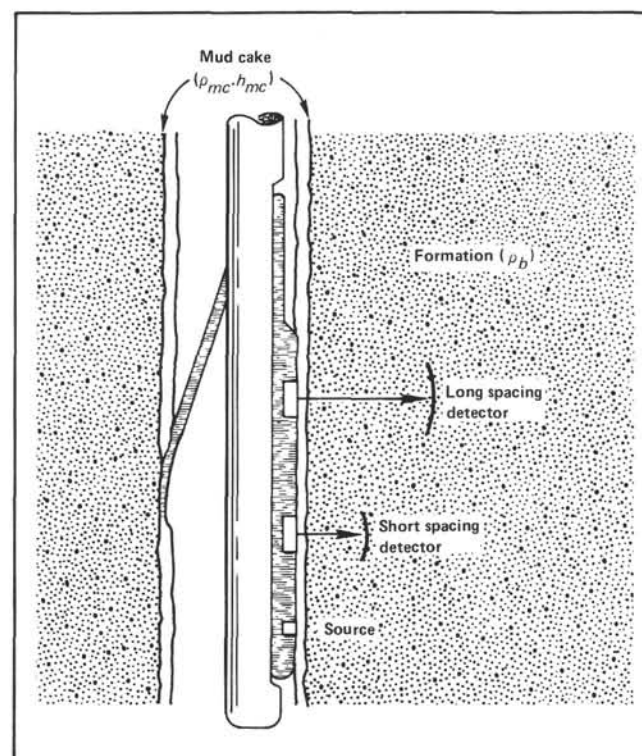


Figure 5. Schematic drawing of the dual spacing Formation Density Logging Device (FDC).

cm<sup>3</sup>, which is in turn dependent on the density of the rock matrix material, the formation porosity, and the density of the fluid filling the pores.

To minimize the influence of borehole fluids, the source and detector mounted on a skid are shielded. The openings of the shields are applied against the borehole wall by means of an eccentricing arm. A correction is needed when the contact between the skid and the formations is poor. In the chart of Figure 6, a plot of long-spacing count rate versus short-spacing count rate is given. Points for a given value of  $\rho_b$  and various hole conditions fall on or close to an average curve. From these average curves, the corrected  $\rho_b$  can be derived without any explicit measurement of hole conditions. This correction is made automatically in the FDC and the corrected  $\rho_b$  and the correction,  $\Delta\rho$ , are recorded on the log.

As a result of the random scattering, the data exhibit statistical variations that are smoothed before recording by passing the signal through a circuit with a time constant adjustable for formation density. The logging speed is chosen so that the tool will not travel more than 1 ft. during one time constant; the maximum recommended logging speed is 1800 ft./hr.

The log data are normally presented with the gamma ray and CNL logs. The density log responds to the electron density of the formations and the electron density,  $\rho_e$ , is proportional to bulk density.

For a substance consisting of a single element,

$$\rho_e = \rho_b \frac{(2Z)}{A}$$

where  $\rho_b$  is the actual bulk density,  $Z$  is the atomic number, and  $A$  is the atomic weight.

For a molecular substance,

$$\rho_e = \rho_b \frac{(2Z's)}{\text{mol. wt.}}$$

where  $Z$  is the sum of the atomic numbers of the atoms in the molecule.

For a density logging tool, calibrated in a fresh-water filled limestone formation, it can be shown that

$$\rho_a = 1.0704 \rho_c - 0.1883$$

where  $\rho_a$  = apparent bulk density recorded by the tool. For sandstones, limestones, and dolomites,  $\rho_a$  is practically identical to the bulk density.

For a clear formation of known matrix density ( $\rho_{ma}$ ), of porosity containing a fluid of average density  $\rho_f$ , the formation bulk density,  $\rho_b$ , is  $\rho_b = \rho_f + (1 - \phi)\rho_{ma}$ .

For many pore fluids the difference between  $\rho_a$  and  $\rho_b$  is small and  $\phi = \rho_{ma} - \rho_b / \rho_{ma} - \rho_f$ , where  $\rho_a = \rho_b$ .

### Gamma Ray (GR)

The gamma-ray log is a measurement of the natural radioactivity of the formations. In sediments, the gamma-ray log is normally a reflection of shale content because radioactive elements are concentrated in clays and shales. The tool also records the gamma-ray activity of the formation through the casing. During Leg 81, the gamma log was used to correlate between the various logging runs.

The gamma-ray sonde contains a scintillation counter to measure the gamma radiation originating in the volume of the formation near the sonde. The naturally radioactive elements contained within the sediments emit gamma rays whose energies are degraded as they pass through the sediment. The amount of absorption depends on the density of the sediment so that less dense sediments will appear to be more radioactive.

The gamma-ray response after correction for hole conditions (diameter, casing, mud weight, etc.) is proportional to the weight concentration of radioactive material in the formation.

The number of gamma rays reaching the counter fluctuates even when the sonde is stationary because of the statistically random natural emission of gamma rays. To average out these statistical variations, various time constants can be selected to accord with the measured level of radioactivity.

It should be noted that in interpreting the gamma-ray curve, a bed boundary is picked at a point halfway between the maximum and minimum deflection. The recorded depth of this point depends on the logging speed and time constant. For example, the apparent depth is shifted in the direction the tool is moving with an increase in the logging speed or length of time constant.

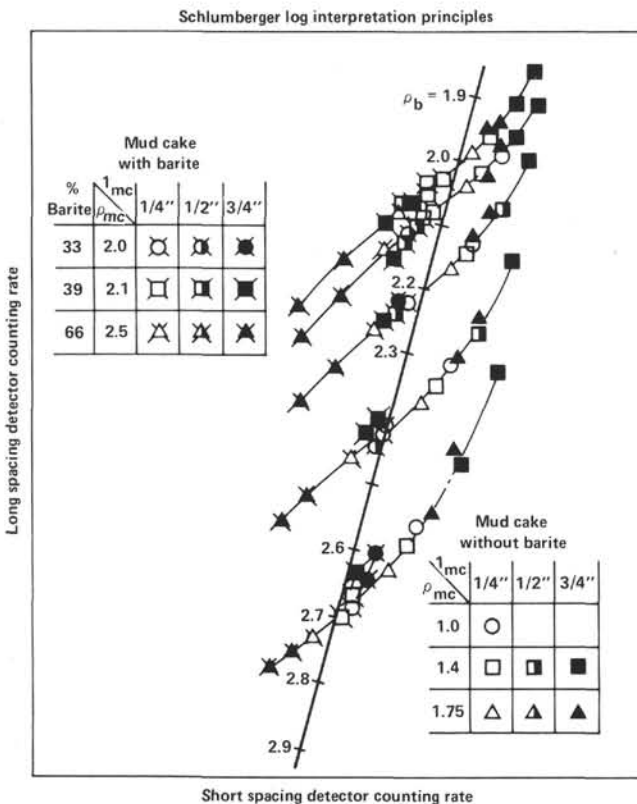


Figure 6. "Spine-and-ribs" plot, showing response of FDC counting rates to mud cake.

The lag is approximately equal to the distance the counter moves during one time constant.

To avoid excessive distortion of the curve, the recording speed is chosen so that the lag is about 1 ft. The dynamic measure point of a gamma-ray logging tool is then taken as being located below the counter at a distance equal to the lag. This places the midpoint of a bed-boundary gamma-ray anomaly at the correct depth on the log.

### Variable Density Log (VDL)

The variable density log provides a qualitative record of the variable amplitude of sonic wave trains transmitted by sonic sondes.

The wave train is displayed on an oscilloscope, the light spot of which varies in brightness in proportion to the amplitude of the received acoustic wave. The oscilloscope traces are photographed onto film moving synchronously with the sonde. On film, amplitude changes are shown by variations in contrast across the film so that dark areas correspond to positive maxima of the wave form.

The amplitude or variable density log is often used to detect fracture systems in hard formations. In such formations, the amplitude of the wave is much reduced. However, bedding planes and thin shale interbeds may give the same response as fractures, so that careful comparison of the logs with core and drilling data is necessary in interpretation. Variations in resistivity and porosity can also determine fracturing.

### Induction Resistivity (ISF)

The induction log was originally developed to measure formation resistivity in boreholes containing oil-based muds. Induction logging devices are focused to reduce the influence of the borehole and of the surrounding formations. The induction sonde consists of several transmitter and receiver coils, but the principles can be understood by considering a sonde comprising a single transmitter and receiver coils (Fig. 7).

A high-frequency alternating current of constant intensity is sent through the transmitter coil, creating an alternating magnetic field that induces secondary currents in the formation. These currents flow in circular ground-loop paths coaxial with the transmitter coil. These ground-loop currents create magnetic fields which induce a current in the receiver coil. The induced current is proportional to the conductivity of the formations. Any signal produced by direct coupling of transmitter and receiver coils is balanced out by the measuring circuits.

The ISF combination used on Leg 81 included a deep induction tool focused to measure the resistivity of the uninvaded zone of the formation and a shallow spherically focused array to measure the resistivity of the flushed and transition zones near the borehole. The spontaneous potential or difference between the potential of a movable electrode in the borehole and the fixed potential of a surface electrode was also measured to calculate formation water resistivity, salinity, and the presence of permeable beds. A gamma-ray log was also run for calibration purposes.

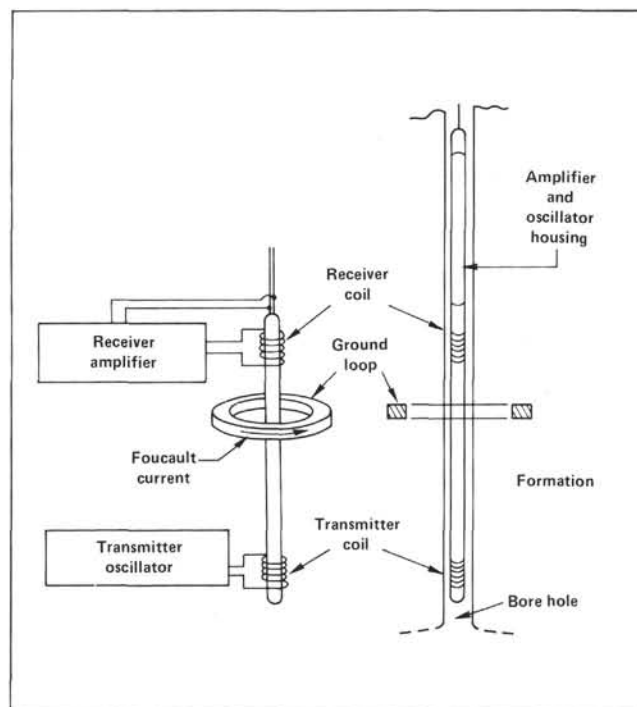


Figure 7. Basic two-coil induction log system

### Operational Aspects of Logging on *Glomar Challenger*

Prior to Leg 48, only logging of re-entry holes had been feasible from *Glomar Challenger*. This was because tools slim enough to pass through the bit were not available, and there was no method of releasing the bit in hole to allow passage of the larger diameter conventional logging tools through the drill stem. For Leg 48, V. Larson, DSDP Operations Manager, developed a special rotary shifting tool to release the bit at the foot of the completed hole, enabling logging of single bit holes. During Leg 81, one re-entry hole was logged and one single bit hole.

After termination of drilling, the holes were prepared for logging by spotting mud and then pulling the drill string back to about 100 m below the sea bed to wipe the hole clean. The drill pipe was then lowered to the terminal depth before the shifting tool was run in to release the bit. After releasing the bit, the drill stem was pulled back to about 100 m below the sea bed. It was necessary to suspend the drill stem at about this depth to support the bottom-hole assembly and bumper subs. In consequence, the upper 100 to 200 m of single bit holes cannot be logged using this technique.

The logging tools were normally run in the following combinations and order: (1) Gamma, Sonic, Caliper; (2) Gamma, Induction SP; (3) Gamma, Neutron, Density.

The logging tools were so contained as to reduce the number of runs and to utilize the gamma log as a correlator between the various runs. During logging, the optical camera was set to run at speeds of 1/200 and 1/1000. A useful complement to the logging was the compilation, during drilling, of a summary lithostratigraphic and physical properties log at a 1/200 scale.

During logging operations, a number of problems were encountered that bear on future logging on *Glomar Challenger*. The DSDP holes are normally drilled using seawater circulation. Although the hole was "wiped clean" and mud was spotted before logging, the tools commonly failed to reach total depth (TD), indicating that the hole was slowly filling. In conventional drilling, using mud circulation, a mud cake would be expected to form a lining to the borehole that would prevent sediment sloughing downhole. Apart from preventing the logs from reaching TD, the poor hole conditions frequently caused "bridging" of the hole, requiring spudding by the tool and, on occasions, fresh wiper runs using the drill stem. A serious effect was to jam the caliper, necessitating care in interpretation. It was found useful to run the caliper downhole to avoid jamming. In future logging, motorized feeler-type calipers may be more useful.

The reliability of several of the logs, notably the density and neutron logs, is dependent on good borehole conditions. In particular, the hole should be smooth and its diameter should not exceed in the 12 in. limit of the eccentricizer used with these tools. Because of jamming, the caliper cannot be reliably used as a check on hole diameter to assess the reliability of these data. However, comparison between these logs, the sonic and resistivity curves, and the small  $\Delta\rho$  values suggest that these logs are reliable. The reliability of the variable density log is questionable, for the required centralization of  $\pm 1/8$  is unlikely to have been achieved.

Wave motion is shown as "stair stepping" on the logs. The effectiveness of the heave compensator in eliminating or reducing wave motion is doubtful and is complicated by the absence of a fixed point of reference once the drill pipe is off the bottom. It should be noted that the 36 in. sheave required by the bending diameter of the Schlumberger cable is too large to be used with the heave compensator. The effects of the heave compensator on logging speed and thus sensor resolution are likely to be variable. A useful addition to the suite of logging tools would be a dipmeter. Taping of the logs is considered an essential part of any logging program on *Glomar Challenger*. Data recorded on tape can be played back in any combination of depth and scale and processed using computer and visual display techniques. Depth adjustments and correlations between logs can be carried out more easily. However, the real data are preserved on tape and can be redisplayed by playback.

It should be noted that depths of the lithostratigraphic log derived from the drillers are usually deeper than those recorded on the electric logs. The magnitude of the discrepancy varies downhole to a maximum of about 9 m and has several causes. The disagreement in the seabed depth arises from small errors ( $\pm 1$  m) in (reading) the echo sounder and the equivocal depth of the first core cut at the sea bed; tidal effects may cause a further discrepancy of  $\pm 1$  m. There are also cumulative errors that arise from the measurement of drill pipe lengths and the uncertain position of the core recovered in each cored interval. Drilled depths determined with the bumper subs closed are also at variance with the drill stem depth determined with the bumper subs open. The problem of correlation between cores and logs could be considera-

bly reduced by routine measurement of the natural gamma-ray activity of the cores using a scanning scintillometer in the laboratory.

In presenting the logs, no attempt has been made to remove these discrepancies, and the lithostratigraphic and electric logs are displayed relative to a common seafloor datum.

Copies of the logs run on Leg 81 may be obtained by writing to the Associate Chief Scientist, Science Services, Deep Sea Drilling Project A-031, University of California at San Diego, La Jolla, California 92093.

### Geochemical Measurements

Aboard ship, analyses for pH, alkalinity, and salinity are conducted routinely.

The pH is determined by two different methods. One is a flow-through electrode method; the other is a punch-in electrode method. pH is determined on all samples via the flow-through method, which is a glass capillary electrode in which a small portion of unfiltered pore water is passed. In the softer sediments a "punch-in" pH is also determined by inserting pH electrodes directly into the sediment at ambient temperature prior to squeezing. The pH electrodes for both methods are plugged into an Orion digital millivolt meter.

Alkalinity is measured by a colorimetric titration of a 1-ml aliquot of interstitial water with 0.1N HCl using a methyl red/blue indicator.

Alkalinity (meq/kg) = (ml HCl titrated) · (97.752).

Salinity is calculated from the fluid refractive index as measured by a Goldberg optical refractometer, using the ratio:

$$\text{Salinity (\text{‰})} = (0.55) \cdot \Delta N$$

where  $\Delta N$  = refractive index difference  $\times 10^4$ . Local surface seawater is regularly examined by each of these methods for reference.

### Quantitative Sedimentologic Analyses

#### Smear Slides

The lithologic classification of sediments is based on visual estimates of texture and composition in smear slides made on board ship. These estimates are of areal abundances on the slide and may differ somewhat from the more accurate laboratory analyses of grain size, carbonate content, and mineralogy. Experience has shown that distinctive minor components can be accurately estimated ( $\pm 1$  or 2%), but that an accuracy of  $\pm 10\%$  for major constituents is rarely attained. Carbonate content is especially difficult to estimate in smear slides, as is the amount of clay present. Smear-slide analyses at selected levels as well as averaged analyses for intervals of uniform lithology are given on the core description sheets. For carbonate content, reference should be made to shipboard carbonate bomb and shore-based analyses.

#### Carbonate Data

During Leg 81, extensive use was made of the carbonate bomb device as an aid in sediment classification on board ship. This device is basically a cylindrical ves-

sel with pressure gauge in which a sediment sample of known weight is reacted with acid. The pressure of  $\text{CO}_2$  generated is measured and converted to percent carbonate. Accuracy to within  $\pm 5\%$  total carbonate has been quoted for the device.

Samples were taken for DSDP shore-based carbon-carbonate analysis using the LECO 70-Second Analyzer. Results of these analyses are shown on the superlogs of each hole, which are to be found in the back pocket to this volume.

### X-Ray Mineralogy Analyses

X-ray mineralogical analyses and studies of Leg 81 sediments were carried out ashore by Latouche and Maillet (this volume) and Desprairies, et al. (this volume). Descriptions of analytical techniques can be found in these chapters. Qualitative shipboard X-ray diffraction studies were made by the shipboard sedimentology group as appropriate. These preliminary on-board results are summarized in each chapter.

### Sediment Induration

The determination of induration is highly subjective, but field geologists have successfully made similar distinctions for many years. The criteria of Moberly and Heath (1971) are used for calcareous deposits; subjective estimate or behavior in core cutting is used for others.

#### 1. Calcareous sediments

Soft: Oozes have little strength and are readily deformed under the finer or the broad blade of a spatula.

Firm: Chalks are partly indurated oozes; they are friable limestones that are readily deformed under the fingernail or the edge of a spatula blade.

Hard: Cemented rocks are termed limestones.

#### 2. The following criteria are used for other sediments:

If the material is soft enough that the core can be split with a wire cutter, the sediment name only is used (e.g., silty clay; sand).

If the core must be cut on the band saw or diamond saw, the suffix "stone" is used (e.g., silty claystone; sandstone).

### Lithologic Classification

The lithologic classification scheme used on Leg 81 is basically that devised by the JOIDES Panel on Sedimentary Petrology and Physical Properties and adopted for use by the JOIDES Planning Committee in March 1974. The classification is descriptive, and sediment/rock names are defined solely on the basis of composition and texture, primary as determined from smear slides, bomb analyses, or under the hand lens on board ship. The classification is outlined below and summarized in Figure 8. Symbols utilized to represent the various sediment types on core description sheets are shown in Figure 9.

#### I. Pelagic Clay

- Less than 20% authigenic components
- Less than 30% siliceous microfossils
- Less than 30%  $\text{CaCO}_3$
- Less than 30% terrigenous components

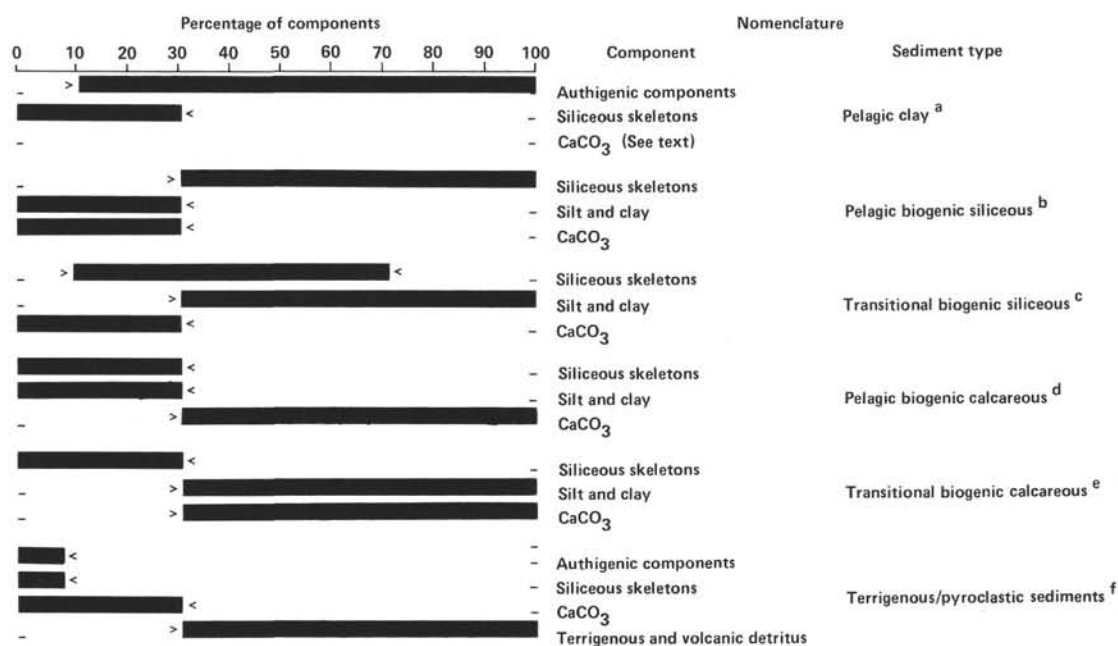
- II. Pelagic Siliceous Biogenic Sediments
  - More than 30% siliceous microfossils
  - Less than 30%  $\text{CaCO}_3$
  - Less than 30% terrigenous components (mud)
  - Radiolarian dominant: radiolarian ooze (or radiolarite)
  - Diatoms dominant: diatom ooze (or diatomite)
  - Sponge spicules dominant: sponge spicule ooze (or spiculite)
  - Where uncertain: siliceous (biogenic) ooze (or chert, porcelanite)
  - When containing 10 to 30%  $\text{CaCO}_3$ : modified by nannofossil, foraminiferal, calcareous, nannofossil-foraminiferal, or foraminiferal-nannofossil, depending upon kind and quantity of  $\text{CaCO}_3$  component.
- III. Transitional Biogenic Siliceous Sediments
  - 10-70% siliceous microfossils
  - 30-90% terrigenous components (mud)
  - Less than 30%  $\text{CaCO}_3$
  - If diatoms less than mud: diatomaceous mud (stone)
  - If diatoms more than mud: muddy diatom ooze (muddy diatomite)
  - If  $\text{CaCO}_3$  10 to 30%: appropriate qualifier is used (see III).
- IV. Pelagic Biogenic Calcareous Sediments
  - More than 30%  $\text{CaCO}_3$
  - Less than 30% terrigenous components
  - Less than 30% siliceous microfossils
  - Principal components are nannofossils and foraminifers; qualifiers are used as follows:

Foram (%)	Name
Less than 10	Nannofossil ooze (chalk, limestone)
10-25	Foraminiferal-nannofossil ooze
25-50	Nannofossil-foraminiferal ooze
More than 50	Foraminiferal ooze

Calcareous sediments containing 10 to 30% siliceous fossils carry the qualifier radiolarian, diatomaceous, or siliceous, depending upon the identification.

#### V. Transitional Biogenic Calcareous Sediments

- More than 30%  $\text{CaCO}_3$
- More than 30% terrigenous components
- Less than 30% siliceous microfossils
- If  $\text{CaCO}_3$ -30 to 60%, marly is used as a qualifier:
  - Soft: marly calcareous (or nannofossil, etc.) ooze
  - Firm: marly chalk (or marly nannofossil chalk, etc.)
  - Hard: marly limestone (or marly nannofossil limestone, etc.)
- If  $\text{CaCO}_3$  is more than 60%:
  - Soft: calcareous (or nannofossil, etc.) ooze
  - Firm: chalk (or nannofossil chalk, etc.)
  - Hard: limestone (or nannofossil limestone, etc.)
- Note: Sediments containing 10 to 30%  $\text{CaCO}_3$  fall in other classes where they are denoted with the adjective "calcareous," "nannofossil," etc.



<sup>a</sup>See descriptive notes in text

<sup>b</sup>Soft—oozes; Hard—radiolarite, diatomite, Chert, or porcellanite

<sup>c</sup>Less than 50% siliceous fossils—diatomaceous (radiolarian) mud or mudstone  
Greater than 50% siliceous fossils—muddy diatom (radiolarian) ooze or muddy diatomite (radiolarite)  
Greater than 10% CaCO<sub>3</sub>—calcareous

<sup>d</sup>Soft—ooze; Firm—chalk; Hard—indurated chalk, limestone

<sup>e</sup>Soft—marly calcareous ooze; Firm—marly chalk; Hard—marly limestone

<sup>f</sup>Soft—clay, mud, silt, sand; Hard—claystone, mudstone, shale (if fissile), siltstone, sandstone  
For pyroclastic sediments see text.

Figure 8. Summary chart of lithologic classification for oceanic sediments.

## VI. Terrigenous Sediments

More than 30% terrigenous components

Less than 30% CaCO<sub>3</sub>

Less than 10% siliceous microfossils

Less than 10% authigenic components

Sediments in this category are subdivided into textural groups on the basis of the relative proportions of three grain-size components: sand, silt, and clay. Sediments coarser than sand-size are treated as "Special Rock Types." The size limits are those defined by Wentworth (1922). The textural classification is according to the triangular diagram shown in Figure 10. The suffix "stone" is used to indicate hard or consolidated equivalents of the unconsolidated sediments.

If CaCO<sub>3</sub> is 10 to 30%, calcareous, nannofossil, etc., is used as a qualifier. Other qualifiers (e.g., feldspathic, glauconitic, tuffaceous, etc.) are used for components more than 10%.

## VII. Pyroclastic Deposits

All sites drilled during Leg 81 encountered pyroclastic deposits. For the purposes of describing this material, we followed the recommendations of the IUGS Subcommittee on the Systematics of Igneous Rocks, as laid out by Schmid (1981). The main criteria utilized by this scheme are grain-size, de-

gree of consolidation, fragmental composition and degree of dilution by nonpyroclastic components, as summarized in Tables 2 and 3.

### Grain-size

Pyroclasts with mean diameters exceeding 64 mm are termed blocks or bombs, those between 2 and 64 mm are lapilli, and those less than 2 mm are ash grains. A further subdivision between coarse and fine ash is made at 1/16 mm, but owing to the difficulty of visually estimating grain size in this range, this subdivision was not used during Leg 81.

### Degree of consolidation

Unconsolidated pyroclastic rocks are termed bomb or block tephra, lapilli tephra, or ashes, depending on grain-size as defined above. The equivalent consolidated rocks are termed agglomerates or pyroclastic breccias, lapilli tuffs, or tuffs.

### Fragmental composition

The prefixes vitric, lithic, or crystal are used to describe the fragmental composition of pyroclastic rocks, depending on the relative abundance of glass or pumice fragments, rock fragments, or crystal particles.

### Nonpyroclastic components

The above terms apply to rocks containing greater than 75% of pyroclasts. If the nonpyroclastic (epi-

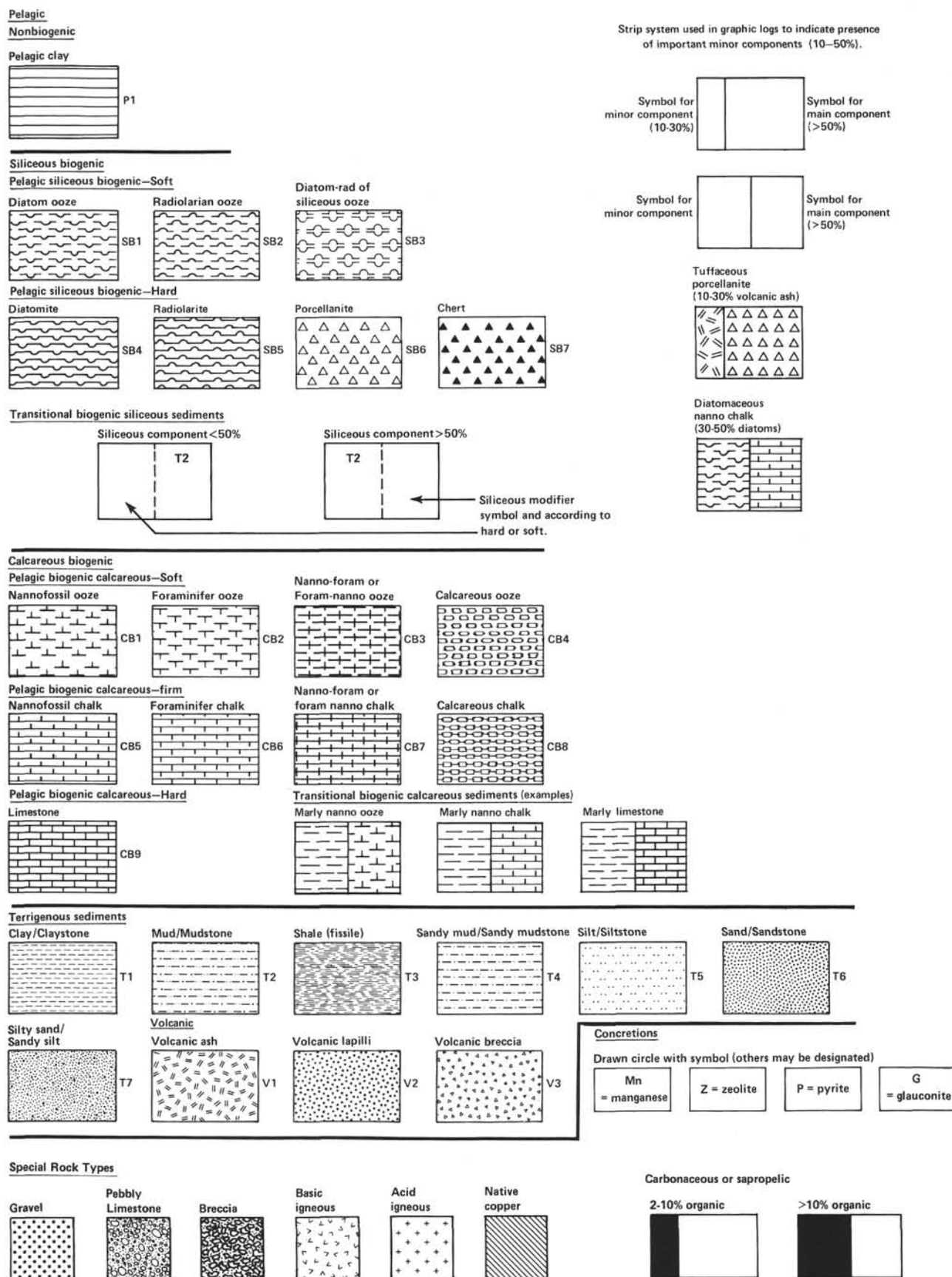


Figure 9. Key to lithologic and biostratigraphic symbols.

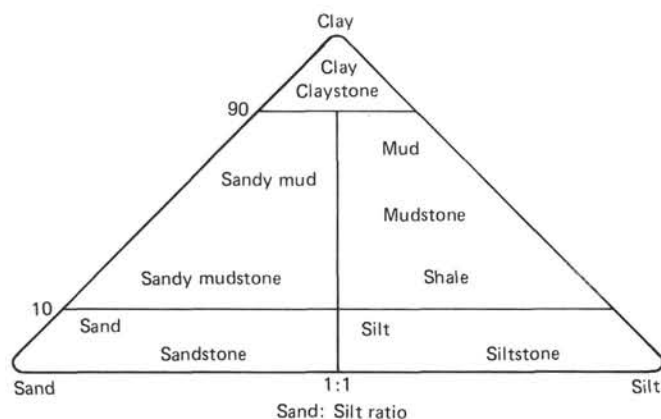


Figure 10. Terminology and class intervals for grade scales. Textural groups-terrigenous sediments.

	Millimeters	Phi ( $\phi$ ) units	Wentworth size class
	2.00	2	1.0 Granule
	1.68	0.75	
	1.41	0.5	Very coarse sand
	1.19	0.25	
	1.00	0.0	
	0.84	0.25	Coarse sand
	0.71	0.5	
	0.59	0.75	
	0.50	1.0	Medium sand
	0.42	1.25	
	0.35	1.5	
	0.30	1.75	
	0.25	2.0	Fine sand
	0.210	2.25	
	0.177	2.5	
	0.149	2.75	
	0.125	3.0	Very fine sand
	0.105	3.25	
	0.088	3.5	
	0.074	3.75	
	0.0625	4.0	
		4.25	Coarse silt
		4.5	
		4.75	
		5.0	Medium silt
		5.25	
		5.5	Fine silt
		5.75	
		6.0	Very fine silt
		6.25	
		6.5	
		6.75	
		7.0	
		7.25	
		7.5	
		7.75	
		8.0	
		8.25	
		8.5	
		8.75	
		9.0	
		9.25	
		9.5	
		9.75	
		10.0	Clay
		10.25	
		10.5	
		10.75	
		11.0	
		11.25	
		11.5	
		11.75	
		12.0	
		12.25	
		12.5	
		12.75	
		13.0	
		13.25	
		13.5	
		13.75	
		14.0	

Table 2. Classification of pyroclastic deposits on the basis of grain size and degree of consolidation.

Clast size	Pyroclast	Pyroclastic deposit	
		Main unconsolidated (tephra)	Mainly consolidated (pyroclastic rock)
64 mm	Bomb, block	Agglomerate, bed of blocks or bomb, block tephra	Agglomerate, pyroclastic breccia
	Lapillus	Layer, bed of lapilli or lapilli tephra	Lapilli tuff
2 mm	Coarse ash grain	Coarse ash	Coarse (ash) tuff
1/16 mm	Fine ash grain (dust grain)	Fine ash	Fine (ash) tuff (dust tuff)

Table 3. Terms for mixed pyroclastic-epiclastic rocks.

Pyroclastic <sup>a</sup>	Tuffites (mixed pyroclastic-epiclastic)	Epiclastic (volcanic and/or nonvolcanic)	Average clast size (mm)
Agglomerate, agglutinate pyroclastic breccia	Tuffaceous conglomerate, Tuffaceous breccia	Conglomerate breccia	64
Lapilli tuff			2
Coarse (Ash) tuff	Tuffaceous sandstone	Sandstone	1/16
Fine	Tuffaceous siltstone, Tuffaceous mudstone, shale	Siltstone, Mudstone, shale	1/256
100%	75%	25%	0% by volume

<sup>a</sup> Terms according to Table 1: — Pyroclasts → Volcanic and nonvolcanic epiclasts (plus minor amounts of biogenic, chemical sedimentary and authigenic constituents).

clastic) content is between 25 and 75% the rock is a tuffite (tuffaceous conglomerate/breccia, sandstone, siltstone, etc.). If the pyroclasts form less than 25%, the rock is considered epiclastic, and the terminology adopted follows that outlined elsewhere in this chapter.

#### IX. Carbonaceous Sediments

Sediments (mudstones, chalks, etc.) containing substantial amounts of detrital plant remains were en-

countered at Site 553. These sediments are indicated as carbonaceous if smear-slide determinations showed the organic content to be greater than 5%, and/or the carbon-carbonate analyses showed greater than 1% by weight of organic carbon.

#### X. Silicified Sediments

At Site 552, much of the calcareous mudstone contains in excess of 10% opaline silica which is not in the form of recognizable microfossils. Very hard layers in this section are classified as chert whereas the somewhat softer portions are termed *silicified* mudstone. The latter are indicated graphically by utilizing the chert symbol in only a fraction of the lithology column. These sediments are thus distinguished from those indicated as *siliceous* wherein greater than 10% of recognizable siliceous microfossils are present, and for which the porcelanite symbol was used.

#### Core Disturbance

Unconsolidated sediments are often quite disturbed by the rotary drilling/coring technique, and there is a complete gradation of disturbance style with increasing sediment induration. An assessment of degree and style of drilling deformation is made on board ship for all cored material, and shown graphically in a separate column on the core description sheets. The following symbols are used:

- — — Slight deformed; bedding contacts slightly bent.
- — — Moderately deformed; bedding contacts have undergone extreme bowing.
- ~~~~~ Highly deformed; bedding completely disturbed, often showing symmetrical diapir-like structures.
- oooooo Soupy, or drilling breccia; water-saturated intervals that have lost all aspects of original bedding and sediment cohesiveness.

Consolidated sediments and rocks seldom show much internal deformation, but are usually broken by drilling into cylindrical pieces of varying length. There is frequently no indication of whether adjacent pieces in the core liner are actually contiguous or whether intervening sediment has been lost during drilling. The symbol  $\bigcirc-\bigcirc$  was used for cylindrical pieces of core separated by intervals of drilling breccia or injected (remolded) softer sediment. In some cases (notably Site 552) fragments of previously drilled material have sloughed back down the hole and been recored. Such material is indicated by the symbol  $(\bigcirc \bigcirc \bigcirc)$  and labeled as *cavings*.

### Sedimentary Structures

Megascopic sedimentary structures are apparent in many of the cored sediments. These include primary features such as lamination, graded bedding, and bioturbation as well as secondary features such as micro-faulting. Where it is reasonably certain that these features are not the product of coring disturbance, they are logged graphically in a separate column on the core description sheets utilizing the symbols shown in Figure 11. Caution should be used in drawing conclusions based on the sedimentary structures because it is often extremely difficult to differentiate between natural structures and those produced by coring.

### Core Description Forms

The basic lithologic and biostratigraphic data are summarized on core description forms (barrel sheets). Insofar as possible, the lithologic data for the main lithology are presented in the following order:

- Sediment or rock name;
- Color name and GSA (or Munsell) number;
- General description of the core, including disturbance, sedimentary structures, and other special features;
- Composition from smear slides and/or thin sections;

Carbon-carbonate determinations;

Grain-size determinations.

Many cores contain important minor lithologies as well as the major lithology, and descriptive information is included for these wherever possible.

An exemplary core description form showing all symbols and explanatory notes is included herewith (Fig. 12) as an aid to understanding and utilizing the core data presented elsewhere in this volume.

### Igneous Rocks

#### Visual Core Description Forms

All igneous rocks were split using a rock saw into working and archive halves described and sampled aboard ship. Figure 13 shows a composite visual core description form used for the description of igneous rocks recovered on Leg 81. On this form, each section of a core is described under a set of five column headings: (1) piece number, (2) graphic representation, (3) orientation, (4) shipboard studies, and (5) alteration.

In the graphic representation column each piece is accurately drawn, and different features, such as texture, glassy margins, or vesicles, are coded according to the symbols given in Figure 14.

Two closely spaced horizontal lines in this column indicate the location of Styrofoam spacers taped between pieces inside the liner. Each piece is numbered sequentially for the entire leg from the top of the first section beginning with the number 1 and continuing in order until the last piece of igneous rock is recovered at the end of the leg. Spacers were placed only between pieces which did not fit together; those pieces were given different numbers. In general, spacers may or may not indicate missing material (not recovered) between pieces.

All cylindrical pieces longer than the diameter of the liner have arrows in the "orientation" column, indicat-

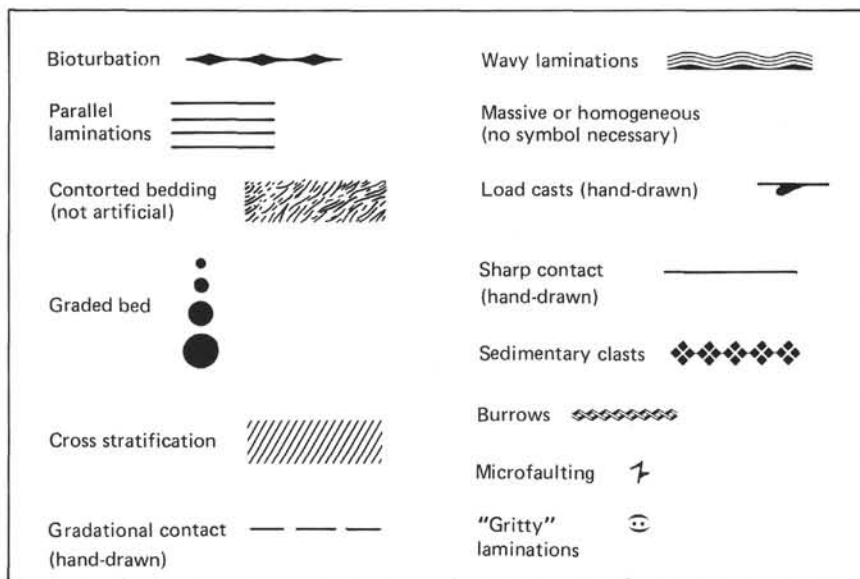


Figure 11. Sedimentary structure symbols.

SITE		HOLE				CORE		CORED INTERVAL:				
TIME-ROCK UNIT	BIOSTRAT ZONE	FOSSIL CHARACTER				SECTION	METERS	GRAPHIC LITHOLOGY	DRILLING DISTURBANCE	SEDIMENTARY STRUCTURES	LITHOLOGIC SAMPLE	LITHOLOGIC DESCRIPTION
		FORAMS	NANNOS	RADS	MICROFACIES							
	(R) Radiolarian Zone	ABUNDANCE A = Abundant C = Common F = Few R = Rare B = Barren				1	0.5 1.0					Color code (GSA and Munsell) plus special remarks  <b>MAJOR LITHOLOGY</b> Color and general description including comments on sedimentary structures, special features of composition, and interbedded minor lithologies.  <u>Smear Slide (SS) and/or Thin Section (TS)*</u> Descriptions Section and depth (2-60) % components  <u>Carbon-Carbonate Determinations</u> Bomb: 2-60 % $\text{CaCO}_3$ LECO: 2-60 % total carbon, % organic carbon, % $\text{CaCO}_3$  <u>Grain Size (shore based)</u> 2-60 % sand, % silt, % clay  <u>X-ray Analysis (see explanatory notes)</u>  Bulk    2-60    <2 $\mu\text{m}$ (partial)    2-60 Qtz,       Smec. Cal,       Ill. Feld,      Kaol. Plag,      Chlor. Other      Zeol. Silica  *TS = In some cases only the rock name is given on the barrel sheet; however, detailed thin section descriptions are listed separately after the barrel sheets for each site.
	(N) Nannoplankton Zone	PRESERVATION G = Good M = Moderate P = Poor				2						
		MICROFACIES See explanatory notes on bio- stratigraphy				3						
						4						
						5						
						6						
						7						
	(F) Foraminiferal Zone					CC						

Figure 12. Sample core description.

[illegible]

Figure 13. Visual core description form for igneous rocks.

ing that top and bottom have not been reversed as a result of drilling and recovery. Arrows also appear on the labels of these pieces on both archive and working halves.

The column marked "Shipboard Studies" designates the location and the type of measurements made on a sample aboard ship. The column headed "Alteration" gives the degree of alteration using the code given in Figure 14. Below each set of five descriptive columns is the designation for core and section for which these data apply. Figure 13 gives the outline for core descriptions of igneous rocks in the right-hand margin of the Visual Core Description Form. If more than one core appears on the core form these data are listed below the description of the first core using the same format. As many cores as space allows are included on one visual core description form. When space for descriptions is inade-

quate on this form, these data appear on the following or facing page. However, in no case does information from one core appear on successive core forms.

For each core, the core number, sections, and depth interval recovered are listed followed by the major and minor rock types and a short description. Thin section data are tallied below this, then shipboard data.

## Classification of Igneous Rocks

We informally classified igneous rocks recovered on Leg 81 according to mineralogy and texture determined from visual inspection of hand specimen and thin sections. The following conventions were agreed upon while at sea, and we realize that they are generalizations. It is possible that gradations may exist within and among textural groups in a single sample.



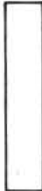
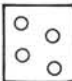








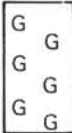


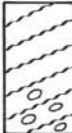


TEXTURE: Used in graphic representation column		WEATHERING ALTERATION Used in alteration column			
	Aphyric basalt		Glass on edge (rounded piece)		Very fresh (no discoloration)
	Olivine phenocrysts		Altered rind on rounded piece		Slightly altered (slight discoloration, with fresh patches)
	Porphyritic basalt		Clinopyroxene phenocrysts		Moderately altered (complete discoloration, major minerals still fresh)
	Plagioclase phenocrysts		Vein with altered zone next to it		Badly altered (discolored, most minerals altered or stained)
	Gabbro		Dolerite		Almost completely altered (completely discolored, beginning to disaggregate, clayey)
	Serpentine (shear orientation approximately as in core; augen shown toward bottom)		Breccia (as graphic as possible)		
	Fractures				

Figure 14. List of symbols for igneous rocks.

Quench textures recognized and described include:

1. Glassy—matrix is basaltic glass with no visible incipient crystallization.
2. Variolitic—texture characterized by the presence of varioles, which are spherical bodies, usually consisting of radiating plagioclase and/or clinopyroxene microlites or crystals; individual crystals are indistinguishable with the microscope.
3. Subvariolitic—texture in which varioles coalesce.
4. Immature sheaf—a bundled arrangement of small crystals (which cannot be individually distinguished with the microscope) assuming a sheaf-like appearance; a central axis of crystal growth often occurs.
5. Mature sheaf—same as above, but discrete skeletal crystals can be distinguished with the microscope (usually greater than 0.005 mm wide).
6. Plumose—plume- or feather-like arrangement of microlites or crystals; may grade from immature to mature (as in sheaf texture) because of crystal size.

Major textural classification for basaltic samples used during Leg 81 include:

1. Phyric—a term describing igneous rocks in which larger crystals (phenocrysts) are set in a finer ground-mass, which may be crystalline or glassy or both.

Aphyric: No phenocrysts  
 Sparsely phyric: 1–2% phenocrysts  
 Moderately phyric: 2–10% phenocrysts  
 Highly phyric: More than 10% phenocrysts

2. Glomerophyric—a term applied to phyric rocks containing clusters of equant crystals larger than the matrix crystals.

3. Ophitic—a term applied to a characteristic of texture in which euhedral or subhedral crystals of plagioclase are embedded in a mesostasis of pyroxene crystals.

4. Subophitic—said of the ophitic texture of an igneous rock in which the feldspar crystals are approximately the same size as the pyroxene and are only partially included by them.

5. Intergranular—a term applied to volcanic rocks in which there is an aggregation of grains of clinopyroxene, not in parallel optical continuity (as in subophitic texture), between a network of feldspar laths which may be diverse, subradial, or subparallel. Intergranular texture is distinguished from an intersertal texture by the absence of interstitial glass or other quenched phases which may fill the interstices between the feldspar laths.

6. Intersertal—a term applied to volcanic rocks in which a base of mesostasis or glass and small crystals fills the interstices between unoriented feldspar laths, the base forming a relatively small proportion of the rock. When the amount of the base increases and the feldspar laths decrease, the texture becomes hyalophitic, and with still greater increase in the amount of the base, the texture becomes hyalopilitic.

Paleomagnetic data taken on board are not listed but will appear in a more comprehensive study by shipboard scientists.

### BIOSTRATIGRAPHY

Definition of an agreed biostratigraphic zonation scheme consistent as far as possible with the magnetostratigraphy is important to promote the essential chronostratigraphy within which the shoreside and shipboard studies can then be interpreted. It is fully recognized that such a scheme may be redefined in the light of further studies that may modify the intercorrelation of foraminifers, nannofossils, diatoms, and radiolarian zones or indeed the age of any at all of these by subsequent magnetostratigraphic studies.

Prior to Leg 81, the Hailwood et al. (1979) bio- and magnetostratigraphic time scale had been developed from the Leg 48 results. Subsequent studies (e.g., Ness, et al., 1980) significantly improved the polarity scale over the interval 0–11.0 m.y. These newer results have required modification of the Hailwood et al. scale. There are also new results in the correlation of diatom zones and the magnetic polarity scale. In view of these new data, a modified version of the Hailwood et al. biostratigraphic and magnetostratigraphic time scale has been adopted (Fig. 15 and Table 4) and is as follows. (See also discussion by Backman et al., this volume.)

1. Magnetic polarity time scale
  - 0–11.0 m.y.: Ness et al. (1980)
  - 11.0–65.0 m.y.: Hailwood et al. (1979)
2. Nannofossils
  - Zonation scheme: Martini (1971)
  - Correlation to polarity scale: 0–11.0 m.y. Berggren and van Couvering (1974)
  - Except for
    - NN19/NN20 } Thierstein et al. (1977)
    - NN20/NN21 }
    - NN15/NN16 } Backman and Shackleton
    - NN16–NN19 } (pers. comm.)
  - 11.0–65.0 m.y. Hailwood et al. (1979)
3. Planktonic Foraminifers
  - Zonation scheme: Blow (1969)
  - Correlation to polarity scale: 0–11.0 m.y. Berggren and van Couvering (1974)
  - 11.0–65.0 m.y. Hailwood et al. (1979)
4. Radiolarians
  - Zonation scheme: Riedel and Sanfilippo (1978)
  - Sphaeropyge langii* Zone (Foreman, 1975); base of zone (Casey and Reynolds, 1980)

Correlation to polarity scale: Theyer et al., 1978

#### 5. Diatoms

Zonation scheme: Burckle (1972, 1977) no diatom zone below the late-middle Miocene has been incorporated into the zonal scheme.

Correlation to polarity scale: Burckle (1972, 1977)

Wherever possible, zone boundaries have been based upon the nominate species of the original zone definition. However, in the Leg 81 area where the nominate species were absent for whatever reason, other species have been used, ranges of which are reasonably well known from areas where they occur together with the nominate species.

Absolute age assignments for the interval 0–11.0 m.y. are taken from Ness et al. (1980) and for 11.0–65.0 from Hailwood et al. (1979).

### REFERENCES

- Berggren, W. A., and Van Couvering, J. A., 1974. Biostratigraphy, geochronology and paleoclimatology of the last 15 m.y. in marine and continental sequences. *Palaeogeogr., Palaeoclimatol., Palaeoecol.*, 16:1–216.
- Blow, W. H., 1969. Late middle Eocene to Recent foraminiferal biostratigraphy. In Brönnimann, P., and Renz, H. H. (Eds.), *Proc. First Int. Conf. Planktonic Microfossils* (Geneva), 1:199–421.
- Boyce, R. E., 1976. Definitions and laboratory techniques of compressional sound velocity parameters and wet-water content, wet-bulk density, and porosity parameters by gravimetric and gamma-ray attenuation techniques. In Schlanger, S. O., Jackson, E. D., et al., *Init. Repts. DSDP*, 33: Washington (U.S. Govt. Printing Office), 931–958.
- Burckle, L. H., 1972. Late Cenozoic planktonic diatom zones from the eastern equatorial Pacific. *Novo Hedwigia Beihefte*, 39:217–246.
- , 1977. Pliocene and Pleistocene diatom datum levels from the equatorial Pacific. *Quat. Geol.*, 7:330–340.
- Casey, R. E., and Reynolds, R. A., 1980. Late Neogene radiolarian biostratigraphy related to magnetostratigraphy and paleoceanography with suggested cosmopolitan radiolarian datums. *Cushman Fdn. Spec. Publ.*, 19:287–300.
- Foreman, H. P., 1975. Radiolaria from the North Pacific, DSDP Leg 32. In Larson, R. L., Moberly, R., et al., 1975. *Init. Repts. DSDP*, 32: Washington (U.S. Govt. Printing Office).
- Hailwood, E. A. Bock, W., et al., 1979. Chronology and biostratigraphy of northeast Atlantic sediments, DSDP Leg 48. In Montadert, L., Roberts, D. G., et al., *Init. Repts. DSDP*, 48: Washington (U.S. Govt. Printing Office), 1119–1141.
- Hinz, K., 1981. A hypothesis on terrestrial catastrophes: Wedges of very thick oceanward dipping layers beneath passive continental margins. *Ecologisches Jahr.*, 22(E):3–28.
- Martini, E., 1971. Standard Tertiary and Quaternary calcareous nannoplankton zonation. *Proc. Second Planktonic Conf.: Rome* (Technoscienza), 2:739–785.
- Matthews, D. J., 1939. *Tables of the Velocity of Sound in Pure Water and in Seawater*: London (Hydrographic Department, Admiralty).
- Moberly, R., Jr., and Heath, G. R., 1971. Carbonate sedimentary rocks from the western Pacific: Leg 7, Deep Sea Drilling Project. In Winterer, E. L., Reidel, W. R., et al., *Init. Repts. DSDP*, 7, Pt. 2: Washington (U.S. Govt. Printing Office), 977–985.
- Montadert, L., Roberts, D. G., et al., 1979. *Init. Repts. DSDP*, 48: Washington (U.S. Govt. Printing Office).
- Morely, J. J., and Shackleton, N. J., 1978. Extension of the radiolarian *Stylatracta universus* as a biostratigraphic datum to the Atlantic Ocean. *Geology*, 6:309–311.
- Ness, G., Levi, S., and Couch, R., 1980. Marine magnetic anomaly time scales for the Cenozoic and Late Cretaceous: A precis, critique, and synthesis. *Rev. Geophys. Space Phys.*, 18:753–770.
- Riedel, W. R., and Sanfilippo, A., 1978. Stratigraphy and evolution of tropical Cenozoic radiolarians. *Microplanktonology*, 24:61–96.
- Schmid, R., 1981. Descriptive nomenclature and classification of pyroclastic deposits and fragments. *Geol. Rundschau*, 70:794–799.

Scientific Staff, 1982. *Glomar Challenger* drills Rockall Plateau. *Geotimes*, 27(9):21-24.

Theyer, F., Mato, C. Y., and Hammond, S. R., 1978. Paleomagnetic and geochronologic calibration of latest Oligocene to Pliocene radiolarian events, equatorial Pacific. *Mar. Micropaleontol.*, 3: 377-395.

Thierstein, H. R., Geitzenauer, K. R., and Molino, B., 1977. Global synchronicity of late Quaternary coccolith datum levels: Validation by oxygen isotopes. *Geology*, 5:400-404.

Wentworth, C. K., 1922. A scale of grade and class terms of clastic sediments. *J. Geol.*, 30:377.

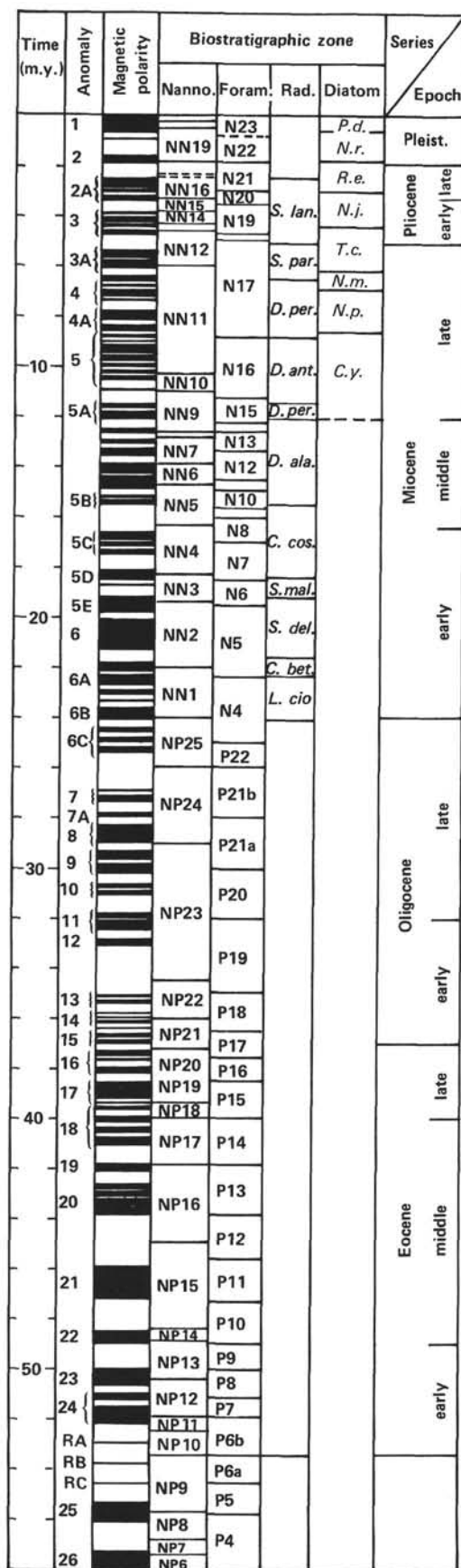
Wentworth, C. K., and Williams, H., 1932. The classification and terminology of the pyroclastic rocks. *Bull. Nat. Res. Council*, (89): 19-53.

Wyllie, M.R. J., Gregory, A. R., and Gardner, G. H. F., 1958. An experimental investigation of factors affecting elastic wave velocities in porous media. *Geophysics*, 23:459.

Wyllie, M.R. J., Gregory, A. R., and Gardner L. W., 1956. Elastic waves in heterogeneous and porous media. *Geophysics*, 21:41.

Table 4. Revised Cenozoic time scale.

Intervals of normal polarity (m.y.)			
Period	Anomaly number	Period	Anomaly number
0.00-0.72	1	22.90-23.08	
0.91-0.97		23.29-23.40	
1.66-1.87	2	23.63-24.07	6B
2.47-2.91	2A	24.41-24.59	6C
2.96-3.07		24.82-24.97	
		25.25-25.43	
3.17-3.40		26.86-26.98	7
3.86-3.98		27.05-27.37	
4.12-4.26		27.83-28.03	
4.41-4.49	3	28.26-28.32	8
4.59-4.79		28.38-28.98	
5.41-5.70		29.31-29.77	9
5.78-6.07	3A	29.82-30.15	
6.42-6.55		30.57-30.82	
6.77-6.86		30.86-31.06	10
6.94-7.34		31.78-32.07	
		32.11-32.45	
7.39-7.44		32.78-33.13	11
7.81-8.18		35.05-35.20	
8.40-8.49		35.25-35.52	13
8.80-8.87	4A	35.83-35.90	
8.98-9.13		35.94-36.01	
		36.07-36.15	14
9.17-9.47		36.37-36.41	
9.48-9.75		36.63-36.80	15
9.78-10.03	5	36.82-36.98	
10.05-10.30		37.32-37.51	
10.42-10.47		37.64-37.87	16
10.89-10.96		37.91-38.24	
11.47-11.66		38.47-39.19	17
11.80-12.09	5A	39.25-39.41	
12.46-12.50		39.47-39.74	
12.59-12.65		39.89-40.24	18
12.88-13.08		40.30-40.64	
13.30-13.58		40.70-41.05	19
13.84-14.28		41.76-42.12	
14.40-14.91		42.60-43.83	
15.13-15.24	5B	45.90-47.18	20
15.42-15.57		48.47-49.02	21
16.63-16.96		50.03-50.69	22
17.00-17.19	5C	51.05-51.24	23
17.27-17.47			24
17.12-18.49		51.47-52.10	
18.72-18.75	5D	55.30-56.06	
19.22-19.80	5E	57.29-57.97	25
20.11-21.31	6	60.87-61.51	26
21.79-22.09	6A	62.47-63.53	27
22.34-22.69		64.00-64.86	28
			29



## Radiolarians

S. u. = last occurrence of *Stylatractus universus*;S. lan. = *Sphaeropyle langii* Zone;S. per. = *Stichocorys peregrina* Zone;D. pen. = *Didymocorys penultima* Zone;D. ant. = *D. antepenultima* Zone;D. pet. = *Diartus petterssoni* Zone;D. ala. = *Dorcadospyris alata* Zone;C. cos. = *Calocycletta costata* Zone;S. wol. = *Stichocorys wolffii* Zone;S. del. = *S. delmontensis* Zone;C. tet. = *Cyrtocapsella tetrapera* Zone;L. elo. = *Lychnoconoma elongata* Zone;D. ate. = *Dorcadospyris ateuchus* Zone;

## Diatoms

P. d. = *Pseudoeunotia deliulus* Zone;N. r. = *Nitzschia reinholdii* Zone;R. p. = *Rhizosolenia praebergonii* Zone;N. j. = *Nitzschia jouseae* Zone;T. c. = *Thalassiosira convexa* Zone;N. m. = *Nitzschia miocenica* Zone;N. p. = *Nitzschia porteri* Zone;C. y. = *Coscinodiscus yabei* Zone;

Figure 15. Bio- and magnetostratigraphic correlations used during Leg 81.